[4] Hawkey CJ. Nonsteroidal anti-inflammatory drug gastropathy. Gastroenterology 2000;119:521–35.
[5] Lichtenberger LM. Where is the evidence that cyclooxygenase inhibition is the primary cause of nonsteroidal anti-inflammatory drug (NSAID)-induced gastrointestinal injury. Topical injury revisited. Biochem Pharmacol 2001;61:631–7.
[6] Whittle BJ. New dogmas or old. Gut 2003;52:1379–81.
[7] Gupta M, Eisen GM. NSAIDs and the gastrointestinal tract. Curr Gastroenterol Rep 2009;11:345–53.
[8] Levine RA, Schwartzel EH. Effect of indomethacin on basal and histamine stimulated human gastric acid secretion. Gut 1984;25:718–22.
[9] Phillipson M, Johansson ME, Henriksnas J, Petersson J, Gendler SJ, Sandler S, et al. The gastric mucus layers: constituents and regulation of accumulation. Am J Physiol Gastrointest Liver Physiol 2008;295:G806–12.
[10] Ligumsky M, Golanska EM, Hansen DG, Kauffman GJ. Aspirin can inhibit gastric mucosal cyclo-oxygenase without causing lesions in rat. Gastroenterology 1983;84:756–61.
[11] Ligumsky M, Sestieri M, Karmeli F, Zimmerman J, Okon E, Rachmilewitz D. Rectal administration of nonsteroidal antiinflammatory drugs Effect on rat gastric ulcerogenicity and prostaglandin E2 synthesis. Gastroenterology 1990;1245–9.
[12] Tanaka K, Tomisato W, Hoshino T, Ishihara T, Namba T, Aburaya M, et al. Involvement of Intracellular Ca2+ Levels in Nonsteroidal Anti-inflammatory Drug-induced Apoptosis. J Biol Chem 2005;280:31059–67.
[13] Tsutsumi S, Gotoh T, Tomisato W, Mima S, Hoshino T, Hwang HJ, et al. Endoplasmic reticulum stress response is involved in nonsteroidal anti-inflammatory drug-induced apoptosis. Cell Death Differ 2004;11:1009–16.
[14] Tomisato W, Tanaka K, Katsu T, Kakuta H, Sasaki K, Tsutsumi S, et al. Membrane permeabilization by non-steroidal anti-inflammatory drugs. Biochem Biophys Res Commun 2004;323:1032–9.
[15] Tomisato W, Tsutsumi S, Rokutan K, Tsuchiya T, Mizushima T. NSAIDs induce both necrosis and apoptosis in guinea pig gastric mucosal cells in primary culture. Am J Physiol Gastrointest Liver Physiol 2001;281:G1092–100.
[16] Aburaya M, Tanaka K, Hoshino T, Tsutsumi S, Suzuki K, Makise M, et al. Heme oxygenase-1 protects gastric mucosal cells against non-steroidal anti-inflammatory drugs. J Biol Chem 2006;281:33422–32.
[17] Tsutsumi S, Namba T, Tanaka KI, Arai Y, Ishihara T, Aburaya M, et al. Celecoxib upregulates endoplasmic reticulum chaperones that inhibit celecoxib-induced apoptosis in human gastric cells. Oncogene 2006;25:1018–29.
[18] Namba T, Hoshino T, Tanaka K, Tsutsumi S, Ishihara T, Mima S, et al. Up-regulation of 150-kDa oxygen-regulated protein by celecoxib in human gastric carcinoma cells. Mol Pharmacol 2007;71:860–70.
[19] Ishihara T, Hoshino T, Namba T, Tanaka K, Mizushima T. Involvement of up-regulation of PUMA in non-steroidal anti-inflammatory drug-induced apoptosis. Biochem Biophys Res Commun 2007;356:711–7.
[20] Tomisato W, Tsutsumi S, Hoshino T, Hwang HJ, Mio M, Tsuchiya T, et al. Role of direct cytotoxic effects of NSAIDs in the induction of gastric lesions. Biochem Pharmacol 2004;67:575–85.
[21] Vane J. Towards a better aspirin. Nature 1994;367:215–6.
[22] Silverstein FE, Faich G, Goldstein JL, Simon LS, Pincus T, Whelton A, et al. Gastrointestinal toxicity with celecoxib vs nonsteroidal anti-inflammatory drugs for osteoarthritis and rheumatoid arthritis: the CLASS study: A randomized controlled trial. Celecoxib Long-term Arthritis Safety Study. JAMA 2000;284:1247–55.
[23] Bombardier C, Laine L, Reicin A, Shapiro D, Burgos VR, Davis B, et al. Comparison of upper gastrointestinal toxicity of rofecoxib and naproxen in patients with rheumatoid arthritis. VIGOR Study Group. N Engl J Med 2000;343:1520–8. 2 p following 8.
[24] FitzGerald GA, Patrono C. The coxibs, selective inhibitors of cyclooxygenase-2. N Engl J Med 2001;345:433–42.
[25] Mukherjee D, Nissen SE, Topol EJ. Risk of cardiovascular events associated with selective COX-2 inhibitors. JAMA 2001;286:954–9.
[26] Mukherjee D. Selective cyclooxygenase-2 (COX-2) inhibitors and potential risk of cardiovascular events. Biochem Pharmacol 2002;63:817–21.
[27] McAdam BF, Catella LF, Mardini IA, Kapoor S, Lawson JA, FitzGerald GA. Systemic biosynthesis of prostacyclin by cyclooxygenase (COX)-2: the human pharmacology of a selective inhibitor of COX-2. Proc Natl Acad Sci USA 1999;96:272–7.
[28] Catella LF, McAdam B, Morrison BW, Kapoor S, Kujubu D, Antes L, et al. Effects of specific inhibition of cyclooxygenase-2 on sodium balance, hemodynamics, and vasoactive eicosanoids. J Pharmacol Exp Ther 1999;289:735–41.
[29] Belton O, Byrne D, Kearney D, Leahy A, Fitzgerald DJ. Cyclooxygenase-1 and -2-dependent prostacyclin formation in patients with atherosclerosis. Circulation 2000;102:840–5.
[30] Yamakawa N, Suemasu S, Kimoto A, Arai Y, Ishihara T, Yokomizo K, et al. Low direct cytotoxicity of loxoprofen on gastric mucosal cells. Biol Pharm Bull 2010;33:398–403.
[31] Misaka E, Yamaguchi T, Iizuka Y, Kamoshida K, Kojima T, Kobayashi K, et al. Anti-inflammatory, Analgesic and Antipyretic Activities of Sodium 2-[4-(2-oxocyclopentan-1-ylmethyl)phenyl] Propionate Dihydrate (CS-600)*. Pharmacometrics 1981;21:753–71.
[32] Kawano S, Tsuji S, Hayashi N, Takei Y, Nagano K, Fusamoto H, et al. Effects of loxoprofen sodium, a newly synthesized non-steroidal anti-inflammatory drug, and indomethacin on gastric mucosal haemodynamics in the human. J Gastroenterol Hepatol 1995;10:81–5.
[33] Sugimoto M, Kojima T, Asami M, Iizuka Y, Matsuda K. Inhibition of prostaglandin production in the inflammatory tissue by loxoprofen-Na, an anti-inflammatory prodrug. Biochem Pharmacol 1991;42:2363–8.
[34] Yamakawa N, Suemasu S, Matoyama M, Kimoto A, Takeda M, Tanaka K, et al. Properties and synthesis of 2-{2-fluoro (or bromo)-4-[(2-oxocyclopentyl)-methyl]phenyl}propanoic acid: nonsteroidal anti-inflammatory drugs with low membrane permeabilizing and gastric lesion-producing activities. J Med Chem 2010;53:7879–82.
[35] Takeuchi K, Ueki S, Okabe S. Importance of gastric motility in the pathogenesis of indomethacin-induced gastric lesions in rats. Dig Dis Sci 1986;31:1114–22.
[36] Tanaka A, Matsumoto M, Hayashi Y, Takeuchi K. Functional mechanism underlying cyclooxygenase-2 expression in rat small intestine following administration of indomethacin: relation to intestinal hypermotility. J Gastroenterol Hepatol 2005;20:38–45.
[37] Asano T, Tanaka K, Yamakawa N, Adachi H, Sobue G, Goto H, et al. HSP70 confers protection against indomethacin-induced lesions of the small intestine. J Pharmacol Exp Ther 2009;330:458–67.
[38] Filaretova L, Tanaka A, Miyazawa T, Kato S, Takeuchi K. Mechanisms by which endogenous glucocorticoid protects against indomethacin-induced gastric injury in rats. Am J Physiol Gastrointest Liver Physiol 2002;283:G1082–89.
[39] Anson ML. The estimation of pepsin, trypsin, papain, and cathepsin with hemoglobin. J Gen Physiol 1938;22:79–89.
[40] Bolton JP, Palmer D, Cohen MM. Stimulation of mucus and nonparietal cell secretion by the E2 prostaglandins. Am J Dig Dis 1978;23:359–64.
[41] Kobayashi I, Kawano S, Tsuji S, Matsui H, Nakama A, Sawaoka H, et al. RGM1, a cell line derived from normal gastric mucosa of rat. In Vitro Cell Dev Biol Anim 1996;32:259–61.
[42] Ohara S, Watanabe T, Hotta K. Comparative study of carbohydrate portion of gastrointestinal mucins using enzyme-linked lectin-binding assay (ELLA). Comp Biochem Physiol B Biochem Mol Biol 1997;116:167–72.
[43] Fujii T, Takahashi Y, Ikari A, Morii M, Tabuchi Y, Tsukada K, et al. Functional association between K + -Cl- cotransporter-4 and H+,K + -ATPase in the apical canalicular membrane of gastric parietal cells. J Biol Chem 2009;284:619–29.
[44] Fujii T, Ohira Y, Itomi Y, Takahashi Y, Asano S, Morii M, et al. Inhibition of P-type ATPases by [(dihydroindenyl)oxy]acetic acid (DIOA), a K+ -Cl- cotransporter inhibitor. Eur J Pharmacol 2007;560:123–6.
[45] Yoda A, Hokin LE. On the reversibility of binding of cardiotonic steroids to a partially purified (Na + K)-activated adenosinetriphosphatase from beef brain. Biochem Biophys Res Commun 1970;40:880–6.
[46] Oner SS, Kaya AI, Onaran HO, Ozcan G, Ugur O. Beta2-Adrenoceptor, Gs and adenylate cyclase coupling in purified detergent-resistant, low density membrane fractions. Eur J Pharmacol 2010;630:42–52.
[47] Ohnishi A, Shimamoto C, Katsu K, Ito S, Imai Y, Nakahari T. EP1 and EP4 receptors mediate exocytosis evoked by prostaglandin E(2) in guinea-pig antral mucous cells. Exp Physiol 2001;86:451–60.
[48] Coleman RA, Smith WL, Narumiya S. International Union of Pharmacology classification of prostanoid receptors: properties, distribution, and structure of the receptors and their subtypes. Pharmacol Rev 1994;46:205–29.
[49] Yamakawa N, Suemasu S, Watanabe H, Tahara K, Tanaka KI, Okamoto Y, et al. Comparison of pharmacokinetics between loxoprofen and its derivative with lower ulcerogenic activity, fluoro-loxoprofen. Drug Metab Pharmacokinet 2012.
[50] Goldstein JL, Eisen GM, Lewis B, Gralnek IM, Aisenberg J, Bhadra P, et al. Small bowel mucosal injury is reduced in healthy subjects treated with celecoxib compared with ibuprofen plus omeprazole, as assessed by video capsule endoscopy. Aliment Pharmacol Ther 2007;25:1211–22.
[51] Aabakken L, Bjornbeth BA, Weberg R, Viksmoen L, Larsen S, Osnes M. NSAID-associated gastroduodenal damage: does famotidine protection extend into the mid- and distal duodenum. Aliment Pharmacol Ther 1990;4:295–303.
[52] Somasundaram S, Sigthorsson G, Simpson RJ, Watts J, Jacob M, Tavares IA, et al. Uncoupling of intestinal mitochondrial oxidative phosphorylation and inhibition of cyclooxygenase are required for the development of NSAID-enteropathy in the rat. Aliment Pharmacol Ther 2000;14:639–50.
[53] Basivireddy J, Vasudevan A, Jacob M, Balasubramanian KA. Indomethacin-induced mitochondrial dysfunction and oxidative stress in villus enterocytes. Biochem Pharmacol 2002;64:339–49.

Biochemical and Biophysical Research Communications 425 (2012) 818–824

Contents lists available at SciVerse ScienceDirect

Biochemical and Biophysical Research Communications

journal homepage: www.elsevier.com/locate/ybbrc

# Expression of 150-kDa oxygen-regulated protein (ORP150) stimulates bleomycin-induced pulmonary fibrosis and dysfunction in mice

Ken-Ichiro Tanaka [a,b], Ayano Shirai [a], Yosuke Ito [b], Takushi Namba [b], Kayoko Tahara [a], Naoki Yamakawa [a,b], Tohru Mizushima [a,b,*]

[a] Department of Analytical Chemistry, Faculty of Pharmacy, Keio University, Tokyo 105-8512, Japan
[b] Faculty of Life Sciences, Kumamoto University, Kumamoto 862-0973, Japan

ARTICLE INFO

*Article history:*
Received 25 July 2012
Available online 7 August 2012

*Keywords:*
ORP150
Bleomycin
IPF
TGF-β1
Myofibroblast

ABSTRACT

Idiopathic pulmonary fibrosis (IPF) involves pulmonary injury associated with inflammatory responses, fibrosis and dysfunction. Myofibroblasts and transforming growth factor (TGF)-β1 play major roles in the pathogenesis of this disease. Endoplasmic reticulum (ER) stress response is induced in the lungs of IPF patients. One of ER chaperones, the 150-kDa oxygen-regulated protein (ORP150), is essential for the maintenance of cellular viability under stress conditions. In this study, we used heterozygous ORP150-deficient mice ($ORP150^{+/-}$ mice) to examine the role of ORP150 in bleomycin-induced pulmonary fibrosis. Treatment of mice with bleomycin induced the expression of ORP150 in the lung. Bleomycin-induced inflammatory responses were slightly exacerbated in $ORP150^{+/-}$ mice compared to wild-type mice. On the other hand, bleomycin-induced pulmonary fibrosis, alteration of lung mechanics and respiratory dysfunction was clearly ameliorated in the $ORP150^{+/-}$ mice. Bleomycin-induced increases in pulmonary levels of both active TGF-β1 and myofibroblasts were suppressed in $ORP150^{+/-}$ mice. These results suggest that although ORP150 is protective against bleomycin-induced lung injury, this protein could stimulate bleomycin-induced pulmonary fibrosis by increasing pulmonary levels of TGF-β1 and myofibroblasts.



## 1. Introduction

Idiopathic pulmonary fibrosis (IPF) is a progressive and devastating chronic lung condition with poor prognosis; the mean length of survival from the time of diagnosis ranges from 2.8 to 4.2 years. No treatment has been shown to improve the prognosis for IPF patients [1]. Recent studies have suggested that lung injury associated with inflammatory responses, transforming growth factor (TGF)-β1 and myofibroblasts play important roles in the pathogenesis of IPF [1,2].

An increase in lung myofibroblasts, an intermediate cell type between fibroblasts and smooth muscle cells, has been suggested to play an important role in the atypical fibrosis and collagen deposition that observed in IPF patients [2]. It was previously thought that the origin of myofibroblasts was solely peribronchiolar and that perivascular fibroblasts transdifferentiate to myofibroblasts in response to various stimuli, in particular TGF-β1 [3]. However, recently it was revealed that lung epithelial cells undergo epithelial–mesenchymal transition (EMT) to become myofibroblasts after treatment with TGF-β *in vitro* [4,5] and that EMT of epithelial cells is induced in the lungs of IPF patients and animals with pulmonary fibrosis (bleomycin-induced pulmonary fibrosis) [4,6,7]. These results suggest that some myofibroblasts in IPF patients are derived from the EMT of lung epithelial cells.

The endoplasmic reticulum (ER) stress response is induced by the accumulation of unfolded and misfolded proteins in the ER [8,9]. ER stress response-related proteins contain not only ER chaperones (such as glucose-regulated protein (GRP)78), that confer protection against stressors by refolding unfolded and misfolded proteins in the ER, but also C/EBP homologous transcription factor, a transcription factor with apoptosis-inducing activity [10]. Since the ER stress response is induced by pathogenic conditions such as hypoxia, inflammation and toxic chemicals, it is not surprising that recent studies have suggested that the ER stress response plays an important role in diseases such as gastric ulcer and Alzheimer's disease [11,12].

*Abbreviations:* BALF, bronchoalveolar lavage fluid; CHOP, C/EBP homologous protein; EMT, epithelial–mesenchymal transition; FVC, forced vital capacity; GRP, glucose-regulated protein; IPF, idiopathic pulmonary fibrosis; MPO, myeloperoxidase; ORP150, 150-kDa oxygen-regulated protein; α-SMA, α-smooth muscle actin; SP-C, surfactant protein C.

* Corresponding author at: Department of Analytical Chemistry, Faculty of Pharmacy, Keio University, 1-5-30, Shibakoen, Minato-ku, Tokyo 105-8512, Japan. Fax: +81 3 5400 2628.
*E-mail address:* mizushima-th@pha.keio.ac.jp (T. Mizushima).

0006-291X/$ - see front matter © 2012 Elsevier Inc. All rights reserved.
http://dx.doi.org/10.1016/j.bbrc.2012.07.158

One of the ER chaperones, the 150-kDa oxygen-regulated protein (ORP150), was originally identified in cultured astrocytes exposed to hypoxia [13]. Previous studies showed that expression of ORP150 is up-regulated under various pathological conditions and this up-regulation is implicated in the progression of these diseases [14,15].

It was recently suggested that IPF also involves the ER stress response, with GRP78 showing increased expression in the lungs of IPF patients and bleomycin-administered mice [16–18]. Genetic studies have revealed that mutations in the gene encoding surfactant protein C (SP-C, a protein produced by lung epithelial cells) could lead to familial interstitial pneumonia (a familial form of IPF) [19,20]. These mutations induce the ER stress response due to the accumulation of misfolded pro-SP-C [16,21]. However, because that induction of the ER stress response was observed in IPF patients without these mutations [16,18], the mechanism and role of ER stress response in IPF patients is unknown at present. Based on the cytoprotective effect provided by ER chaperones, it was considered that they would have a negative impact on the development of IPF (i.e. protective roles against IPF); however, no direct evidence (such as genetic evidence) exists to substantiate this. On the other hand, it was recently reported that the ER stress response stimulates the myofibroblastic differentiation of fibroblasts and EMT of lung epithelial cells *in vitro* [18,22]. Therefore, it is also possible that the ER stress response has a positive influence on the development of IPF. Thus, to understand the role of ER stress response in IPF, it may prove useful in the first instance to examine artificially induced pulmonary fibrosis in transgenic mice expressing each protein related to the response.

In line with this, we compare here aspects of bleomycin-induced pulmonary fibrosis in heterozygous ORP150-deficient mice ($ORP150^{+/-}$ mice) and wild-type mice. Bleomycin-induced pulmonary inflammatory responses were slightly exacerbated, while pulmonary fibrosis and dysfunction were clearly ameliorated in $ORP150^{+/-}$ mice compared to wild-type mice. We also found that bleomycin-induced increases in the pulmonary levels of both active TGF-β1 and myofibroblasts were suppressed in $ORP150^{+/-}$ mice. These results suggest that ORP150 is stimulative for bleomycin-induced pulmonary fibrosis, though at the same time ORP150 exerts a protective action against bleomycin-induced lung damage.

## 2. Materials and methods

### 2.1. Animals

Mice heterozygous for a truncated/inactivated mutant form of ORP150 ($ORP150^{+/-}$) and their wild-type counterparts ($ORP150^{+/+}$) (6–8 weeks of age) were prepared as described previously [12]. The experiments and procedures described here were carried out in accordance with the Guide for the Care and Use of Laboratory Animals as adopted and promulgated by the National Institutes of Health, and were approved by the Animal Care Committee of Keio University and Kumamoto University.

### 2.2. Administration of bleomycin, preparation of bronchoalveolar lavage fluid (BALF), assay for MPO activity, analysis of lung function and histological and immunohistochemical analyses

Mice were maintained under anaesthesia with chloral hydrate (500 mg/kg) and were given one intratracheal injection of bleomycin (5 mg/kg) to induce pulmonary fibrosis.

BALF was collected by cannulating the trachea and lavaging the lung with 1 ml of sterile PBS containing 50 units/ml heparin (two times). The total cell number in the BALF was counted using a haemocytometer. Cells were stained with Diff-Quik reagents and the ratios of alveolar macrophages, lymphocytes and neutrophils to total cells were determined. More than 200 cells were counted for each sample.

Myeloperoxidase (MPO) activity in the lung was measured as described previously [23].

Analysis of lung function was performed with a computer-controlled small-animal ventilator (FlexiVent; SCIREQ, Montreal, Canada) as described previously [24].

Histological and immunohistochemical analyses were done as described previously [24].

### 2.3. Hydroxyproline determination and ELISA for active TGF-β1

Hydroxyproline content was determined as described [25]. The active TGF-β1 content in the lung was determined by ELISA as described previously [24].

### 2.4. Immunoblotting analysis and real-time RT-PCR analysis

Total protein was prepared as described previously [26]. Samples were applied to polyacrylamide SDS gels and subjected to electrophoresis, after which the proteins were immunoblotted with an antibody against ORP150.

Real-time RT-PCR was performed as previously described [27]. The primers used were (name: forward primer, reverse primer): *Orp150*: 5′-gaagatgcagagcccatttc-3′, 5′-tctgctccaggacctcctaa-3′; *α-sma*: 5′-catcatgcgtctggatctgg-3′, 5′-ggacaatctcacgctcagca-3′; *E-cadherin*: 5′-tgcccagaaaatgaaaaagg-3′, 5′-gtgtatgtggcaatgcgttc-3′; *Col1a1*: 5′-ccctgtctgcttcctgtaaact-3′, 5′-catgttcggttggtcaaagata-3′; *actin*: 5′-ggacttcgagcaagagatgg-3′, 5′-agcactgtgttggcgtacag-3′.

### 2.5. Transfection

The siRNA for ORP150 was purchased from Qiagen. Cells were transfected with the siRNA using HiPerFect transfection reagents (Invitrogen) according to the manufacturer's instructions.

The plasmid for overexpression of ORP150 was constructed by insertion of the *Orp150* gene in pCI-neoORP150 [28] into pcDNA3.1 (Invitrogen). The transfection was carried out using Lipofectamine LTX (Invitrogen).

### 2.6. Statistical analysis

All values are expressed as the mean ± S.E.M. or S.D. Two-way analysis of variance followed by the Tukey test was used to evaluate differences between more than three groups. Differences were considered to be statistically significant for values of $p < 0.05$.

## 3. Results

### 3.1. Effect of down-regulation of ORP150 expression on bleomycin-induced pulmonary inflammatory responses

Pulmonary inflammation and fibrosis were induced by a once-only (at day 0) intratracheal administration of bleomycin, as described previously [25]. First, we monitored the expression of ORP150 in lung tissues by immunoblotting. As shown in Fig. 1A–D, treatment of mice with bleomycin increased the pulmonary level of ORP150 in $ORP150^{+/-}$ mice and wild-type mice, though the $ORP150^{+/-}$ mice showed lower ORP150 expression than the wild-type mice both in the presence and absence of bleomycin treatment.

The bleomycin-induced inflammatory response can be monitored in terms of the number of inflammatory cells in BALF after the administration of bleomycin [25]. As shown in Fig. 2A, the total

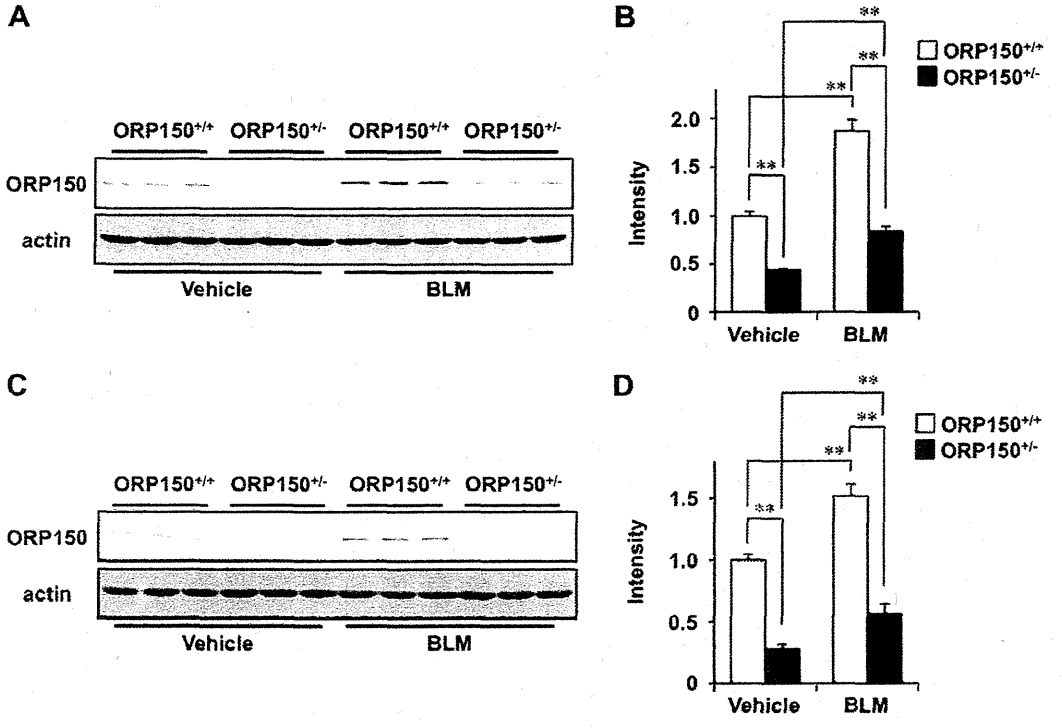


**Fig. 1.** Bleomycin-induced expression of ORP150 in the lung. ORP150$^{+/-}$ mice and wild-type mice (ORP150$^{+/+}$) were treated with (BLM) or without (Vehicle) bleomycin (5 mg/kg) once-only on day 0. Lungs were excised on day 3 (A and B) or 14 (C and D). Tissue homogenates were analysed by immunoblotting with antibodies against ORP150 or actin (A and C). The band intensity of ORP150 was determined and normalised to actin intensity (B and D). Values are mean ± S.E.M. ($n = 3$). $^{**}p < 0.01$. Scale bar, 50 μm.

number of inflammatory cells and individual numbers of alveolar macrophages, lymphocytes and neutrophils were all increased on day 3 after the bleomycin treatment. Compared to wild-type mice, this increase was slightly enhanced in ORP150$^{+/-}$ mice (Fig. 2A). Similar results were observed for MPO activity, an indicator of the inflammatory infiltration of leucocytes (Fig. 2B). These results suggest that ORP150 expression protects against bleomycin-induced inflammatory response.

### 3.2. Effect of down-regulation of ORP150 expression on bleomycin-induced pulmonary fibrosis, alteration of lung mechanics and respiratory dysfunction

Bleomycin-induced pulmonary fibrosis can be assessed by histopathological analysis and measurement of hydroxyproline levels. Haematoxylin and eosin (H & E) staining and Masson's trichrome staining of collagen revealed that bleomycin-induced collagen deposition was less apparent in ORP150$^{+/-}$ mice than in wild-type mice (Fig. 3A and B). Bleomycin also increased pulmonary hydroxyproline levels, although to a lesser degree in the ORP150$^{+/-}$ mice compared with wild-type mice (Fig. 3C). These results suggest that bleomycin-induced pulmonary fibrosis is less extensive in ORP150$^{+/-}$ mice compared to wild-type mice.

We then examined the effect of ORP150 expression on bleomycin-induced alterations of lung mechanics using a computer-controlled small-animal ventilator. Total respiratory system elastance (elastance of total lung including bronchi, bronchioles and alveoli) and tissue elastance (elastance of alveoli) were indistinguishable between heterozygous and wild-type mice in the absence of bleomycin treatment (Fig. 3D). In contrast, both types of mice showed increases in these parameters in response to bleomycin treatment, with this effect being more prominent in wild-type mice. These results suggest that the bleomycin-induced alteration of lung mechanics is ameliorated by the down-regulation of ORP150 expression.

As shown in Fig. 3E, FVC was indistinguishable between vehicle-treated ORP150$^{+/-}$ and wild-type mice, but was clearly decreased by the bleomycin treatment in wild-type mice while remaining unchanged in ORP150$^{+/-}$ mice (Fig. 3E). These results suggest that ORP150 expression exacerbates bleomycin-induced respiratory dysfunction.

To elucidate the mechanism underlying this stimulative effect of ORP150 on pulmonary fibrosis, we focused our attention on myofibroblast and TGF-β1. As shown in Fig. 4A, a bleomycin-dependent increase in the expression of α-SMA, a myofibroblast marker, was suppressed in ORP150$^{+/-}$ mice compared to wild-type mice, suggesting that the expression of ORP150 stimulates an increase in pulmonary myofibroblast number in the presence of bleomycin.

As shown in Fig. 4B, active TGF-β1 was increased by the bleomycin treatment; however the level was lower in ORP150$^{+/-}$ mice than in wild-type mice. These results suggest that ORP150 expression also stimulates a bleomycin-dependent increase in active TGF-β1 in lung tissue.

### 3.3. Effect of ORP150 expression on the TGF-β1-induced EMT of epithelial cells and differentiation of fibroblasts in vitro

As described in Section 1, an increase in pulmonary myofibroblasts associated with fibrosis is due to the stimulation of EMT of epithelial cells and the myofibroblastic differentiation of fibroblasts. We tested whether the expression of ORP150 affects these phenomena by examining *in vitro* the effect of siRNA for ORP150 on the TGF-β1-dependent alteration of expression of EMT-related genes in cultured human type II alveolar (A549) cells. Treatment of cells with TGF-β1 down-regulated the expression of the epithelial cell

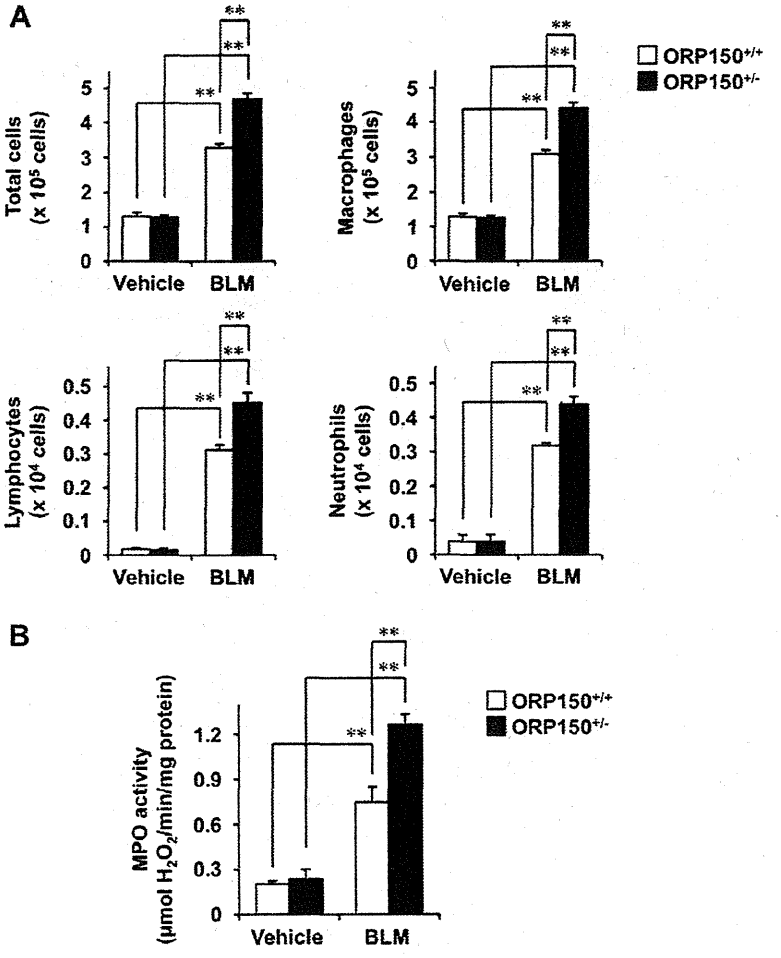


**Fig. 2.** Effect of down-regulation of ORP150 expression on bleomycin-induced pulmonary inflammatory responses. ORP150$^{+/-}$ mice and wild-type mice (ORP150$^{+/+}$) were treated with (BLM) or without (Vehicle) bleomycin (5 mg/kg) once-only on day 0 and lung tissue or BALF was obtained on day 3. Total cell number and individual numbers of alveolar macrophages, lymphocytes and neutrophils in BALF were counted (A). MPO activities in lung homogenates were determined (B). Values are mean ± S.E.M. $^{**}p < 0.01$.

marker *E-cadherin* mRNA (Fig. 4C), suggesting that TGF-β1 induces the EMT-like phenotype of A549 cells. Transfection of cells with siRNA for ORP150 suppressed the expression of *Orp150* mRNA but did not affect the expression of *E-cadherin* mRNA in the presence or absence of TGF-β1 (Fig. 4C). These results suggest that ORP150 expression does not affect the EMT of lung epithelial cells.

We also examined the effect of ORP150 expression on TGF-β1-dependent myofibroblastic differentiation of fibroblasts *in vitro*. Treatment of human embryonic lung fibroblasts (HFL-1 cells) with TGF-β1 induced the expression of α-*sma* and *col1a1* mRNAs (Fig. 4D), suggesting that TGF-β1 activates the transition of fibroblasts to myofibroblasts. The transfection of cells with siRNA for ORP150 slightly decreased the expression of α-*sma* and *col1a1* mRNAs in the presence of TGF-β1 (Fig. 4D). We then examined the effect of overexpression of ORP150 on the myofibroblastic differentiation of fibroblasts. As shown in Fig. 4E, slightly increased the expression of α-*sma* and *col1a1* mRNAs was observed in the presence of TGF-β1. These results suggest that ORP150 expression stimulates the TGF-β1-dependent myofibroblastic differentiation of fibroblasts.

## 4. Discussion

Pulmonary fibrosis is triggered by pulmonary damage and inflammatory responses. In other words, pulmonary fibrosis is a result of abnormal and extended repair and remodelling of damaged lung tissues. We here showed that bleomycin-induced inflammatory responses, such as an increase in BALF leucocyte number and activation of pulmonary MPO, were stimulated in ORP150$^{+/-}$ mice, suggesting that expression of ORP150 could suppress inflammatory responses. As such, we postulated that bleomycin-induced pulmonary fibrosis would be exacerbated in ORP150$^{+/-}$ mice. However, surprisingly, this was not the case. Further to this, we found that increases in pulmonary levels of both active TGF-β1 and myofibroblasts in response to bleomycin were suppressed in ORP150$^{+/-}$ mice compared to wild-type mice. These results suggest that although expression of ORP150 is protective against bleomycin-induced inflammatory responses, it could accentuate pulmonary fibrosis by increasing pulmonary levels of TGF-β1 and myofibroblasts.

As described above, it was recently reported that induction of the ER stress response by chemicals or by expression of misfolded proteins in the ER in alveolar endothelial cells or fibroblasts causes EMT or myofibroblastic differentiation, respectively [18,22]. Therefore, it is possible that the up-regulation of ORP150 expression is responsible for the observed results. We tested this idea *in vitro* and found that the TGF-β1-dependent induction of EMT-like phenotypes in lung epithelial cells was not affected by the suppression of ORP150 expression. On the other hand, the TGF-β1-dependent activation of fibroblasts (myofibroblastic differentiation) was

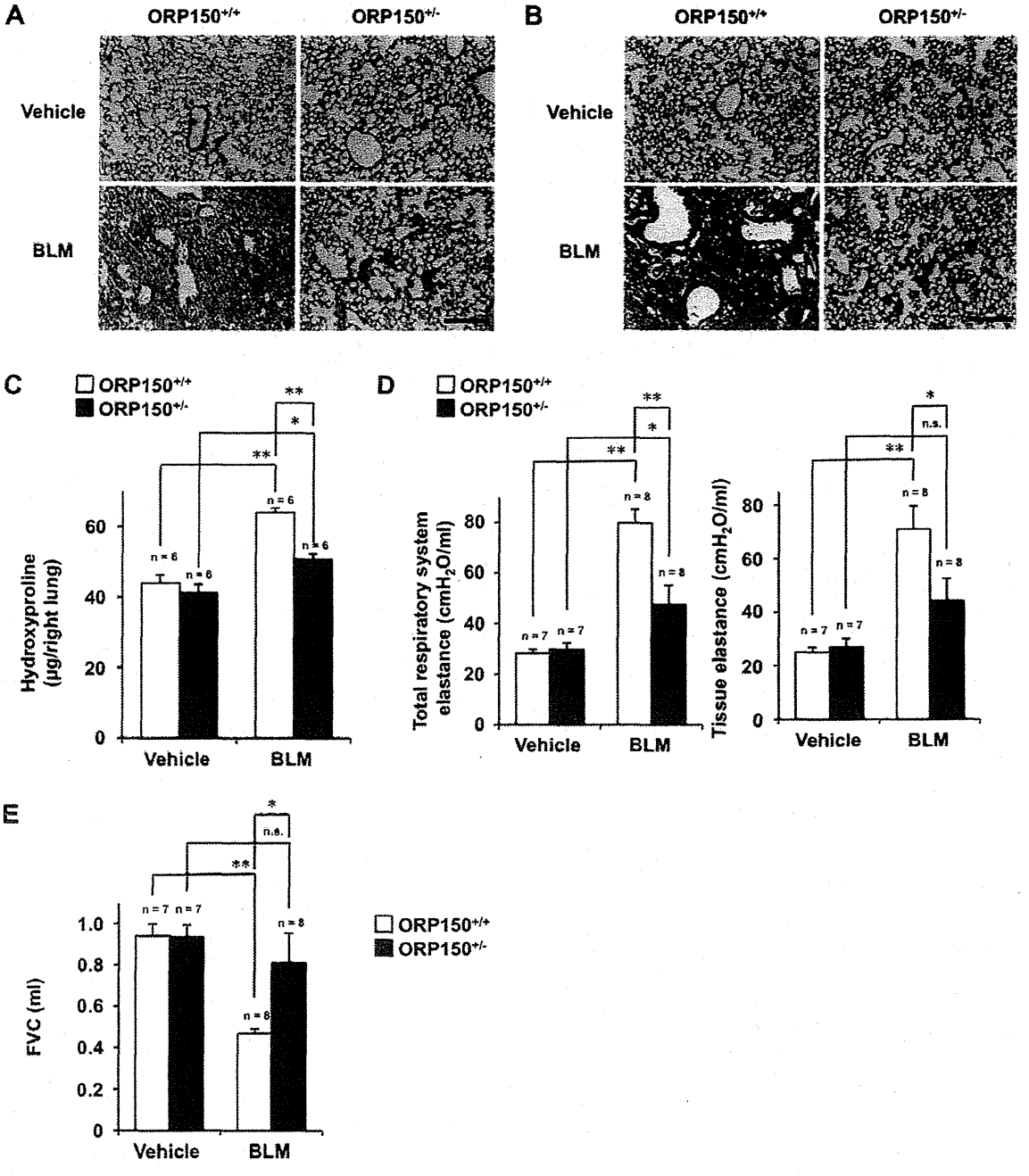


**Fig. 3.** Effect of down-regulation of ORP150 expression on bleomycin-induced pulmonary fibrosis, alteration of lung mechanics and respiratory dysfunction. ORP150$^{+/-}$ mice and wild-type mice (ORP150$^{+/+}$) were treated with (BLM) or without (Vehicle) bleomycin (5 mg/kg) once-only on day 0 and lung tissue removed on day 14. Sections of pulmonary tissue were subjected to H & E staining (A) or Masson's trichrome staining (B). Pulmonary hydroxyproline levels in lung homogenates were determined (C). Total respiratory system elastance (D), tissue elastance (D) and FVC (E) were determined on day 14. Values shown are mean ± S.E.M. $^{**}p < 0.01$; $^{*}p < 0.05$. Scale bar, 100 μm.

slightly suppressed or stimulated by the suppression or induction, respectively, of ORP150 expression. These results suggest that ORP150 expression stimulates the increase in lung myofibroblasts by stimulating myofibroblastic differentiation rather than by stimulating the EMT of epithelial cells.

Although assessment tools used in bleomycin-induced pulmonary fibrosis are primarily based on histological and quantitative collagen analysis, the clinical management of IPF relies on lung function analysis. We therefore used a computer-controlled small-animal ventilator to monitor the effect of bleomycin on elastance, as an increase in elastance has also been associated with human IPF [29]. We found that the bleomycin-induced alteration of lung mechanics was ameliorated in ORP150$^{+/-}$ mice compared to wild-type mice. An improvement of FVC serves as the endpoint of clinical assessments to estimate the efficacy of candidate drugs in IPF patients; to this extent we found that bleomycin-induced a decrease in FVC was ameliorated in ORP150$^{+/-}$ mice compared to wild-type mice. These results suggest that ORP150 expression stimulates not only bleomycin-induced pulmonary fibrosis but also alters lung mechanics and respiratory dysfunction.

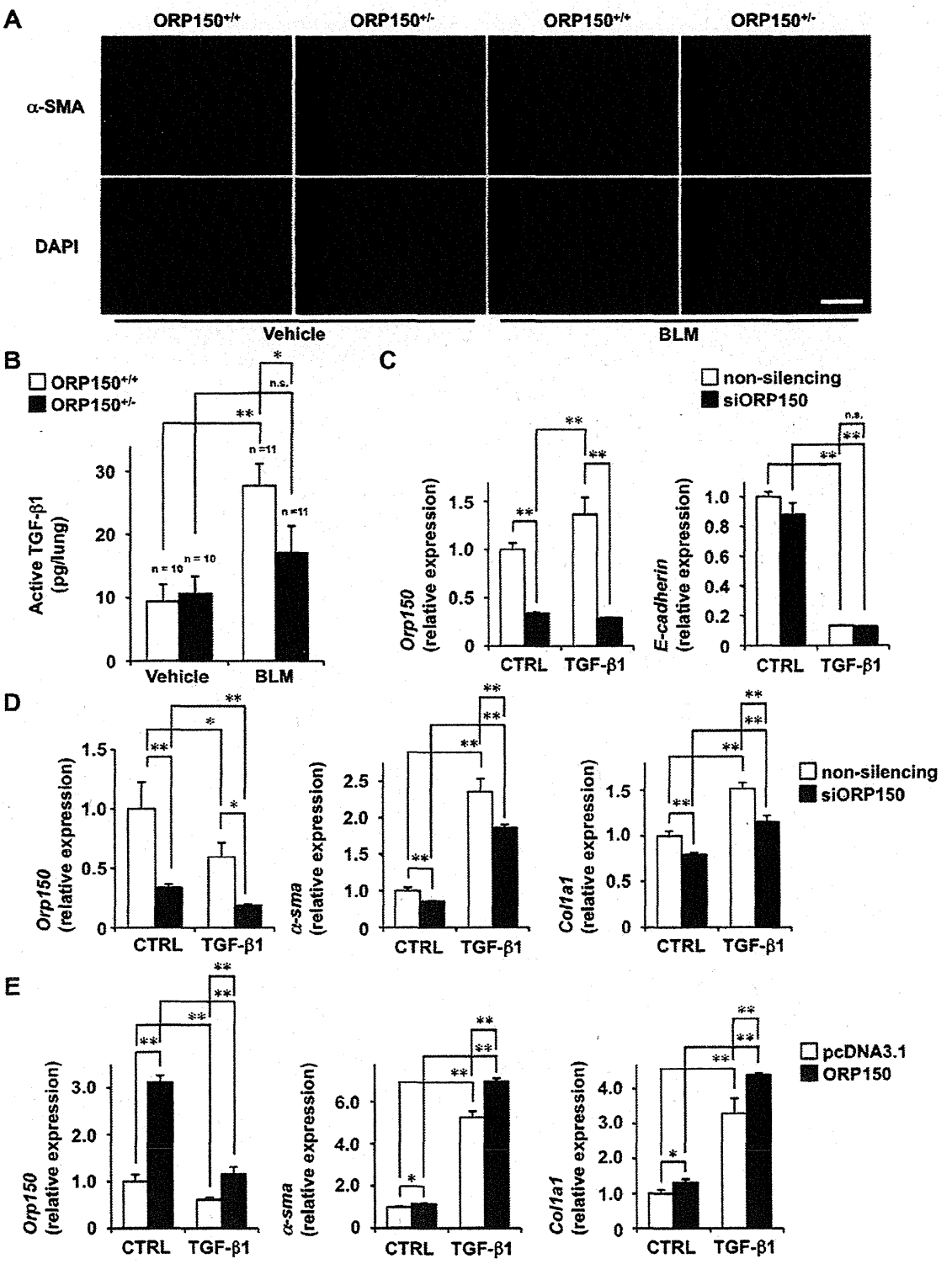


**Fig. 4.** Effect of down-regulation of ORP150 expression on the pulmonary levels of myofibroblasts and active TGF-β1 *in vivo* and on TGF-β1-induced EMT-like phenotypes of epithelial cells and myofibroblastic differentiation of fibroblasts *in vitro*. (A and B) ORP150$^{+/-}$ mice and wild-type mice (ORP150$^{+/+}$) were treated with (BLM) or without (Vehicle) bleomycin (5 mg/kg) once-only on day 0 and lung tissues removed on day 7 (B) or 14 (A). Sections of pulmonary tissue were subjected to immunohistochemical analysis with an antibody against α-SMA (A). Levels of active TGF-β1 in lung homogenates were measured by ELISA (B). Values shown are mean ± S.E.M. $^{**}p < 0.01$; $^{*}p < 0.05$. Scale bar, 50 μm. (C–E) A549 (C) or HFL-1 (D) cells were transfected with 1.0 μg of siRNA for ORP150 (siORP150) or non-silencing siRNA and incubated for 24 h (C and D). HFL-1 cells were transiently transfected with 2.5 μg of expression plasmid for ORP150 or control vector (pcDNA3.1) and cultured for 24 h (E). Cells were then incubated with 10 ng/ml TGF-β1 for 24 (D and E) or 48 h (C). Total RNA was extracted and subjected to real-time RT-PCR using a specific primer set for each gene. Values were normalised to the *actin* gene and expressed relative to the control sample. Values shown are mean ± S.E.M. ($n = 3$). $^{**}p < 0.01$; $^{*}p < 0.05$.

Taken together, the findings presented here suggest that ORP150 could serve as a possible drug target for IPF; however, this requires careful examination given that drugs that inhibit ORP150 function may also induce acute lung injury by suppressing the cytoprotective effects that ORP150 exerts against pulmonary damage.

## Acknowledgments

This work was supported by Grants-in-Aid for Scientific Research from the Ministry of Health, Labour, and Welfare of Japan, as well as the Japan Science and Technology Agency and Grants-in-Aid for Scientific Research from the Ministry of Education, Culture, Sports, Science and Technology, Japan.

## References

[1] American Thoracic Society, Idiopathic pulmonary fibrosis: diagnosis and treatment. International consensus statement. American Thoracic Society (ATS), and the European Respiratory Society (ERS), Am. J. Respir. Crit. Care Med. 161 (2000) 646–664.
[2] D. Sheppard, Transforming growth factor beta: a central modulator of pulmonary and airway inflammation and fibrosis, Proc. Am. Thorac. Soc. 3 (2006) 413–417.
[3] T. Kisseleva, D.A. Brenner, Fibrogenesis of parenchymal organs, Proc. Am. Thorac. Soc. 5 (2008) 338–342.
[4] B.C. Willis, Z. Borok, TGF-beta-induced EMT: mechanisms and implications for fibrotic lung disease, Am. J. Physiol. Lung Cell. Mol. Physiol. 293 (2007) L525–534.
[5] U. Bartram, C.P. Speer, The role of transforming growth factor beta in lung development and disease, Chest 125 (2004) 754–765.
[6] K.K. Kim, M.C. Kugler, P.J. Wolters, L. Robillard, M.G. Galvez, A.N. Brumwell, D. Sheppard, H.A. Chapman, Alveolar epithelial cell mesenchymal transition develops in vivo during pulmonary fibrosis and is regulated by the extracellular matrix, Proc. Natl. Acad. Sci. USA 103 (2006) 13180–13185.
[7] Z. Wu, L. Yang, L. Cai, M. Zhang, X. Cheng, X. Yang, J. Xu, Detection of epithelial to mesenchymal transition in airways of a bleomycin induced pulmonary fibrosis model derived from an alpha-smooth muscle actin-Cre transgenic mouse, Respir. Res. 8 (2007) 1.
[8] R.J. Kaufman, Orchestrating the unfolded protein response in health and disease, J. Clin. Invest. 110 (2002) 1389–1398.
[9] D. Ron, Translational control in the endoplasmic reticulum stress response, J. Clin. Invest. 110 (2002) 1383–1388.
[10] H. Zinszner, M. Kuroda, X. Wang, N. Batchvarova, R.T. Lightfoot, H. Remotti, J.L. Stevens, D. Ron, CHOP is implicated in programmed cell death in response to impaired function of the endoplasmic reticulum, Genes Dev. 12 (1998) 982–995.
[11] T. Hoshino, T. Nakaya, W. Araki, K. Suzuki, T. Suzuki, T. Mizushima, Endoplasmic reticulum chaperones inhibit the production of amyloid-beta peptides, Biochem. J. 402 (2007) 581–589.
[12] T. Namba, T. Hoshino, S. Suemasu, M. Takarada-Iemata, O. Hori, N. Nakagata, A. Yanaka, T. Mizushima, Suppression of expression of endoplasmic reticulum chaperones by *Helicobacter pylori* and its role in exacerbation of non-steroidal anti-inflammatory drug-induced gastric lesions, J. Biol. Chem. 285 (2010) 37302–37313.
[13] K. Kuwabara, M. Matsumoto, J. Ikeda, O. Hori, S. Ogawa, Y. Maeda, K. Kitagawa, N. Imuta, T. Kinoshita, D.M. Stern, H. Yanagi, T. Kamada, Purification and characterization of a novel stress protein, the 150-kDa oxygen-regulated protein (ORP150), from cultured rat astrocytes and its expression in ischemic mouse brain, J. Biol. Chem. 271 (1996) 5025–5032.
[14] K. Ozawa, M. Miyazaki, M. Matsuhisa, K. Takano, Y. Nakatani, M. Hatazaki, T. Tamatani, K. Yamagata, J. Miyagawa, Y. Kitao, O. Hori, Y. Yamasaki, S. Ogawa, The endoplasmic reticulum chaperone improves insulin resistance in type 2 diabetes, Diabetes 54 (2005) 657–663.
[15] T. Nakagomi, O. Kitada, K. Kuribayashi, H. Yoshikawa, K. Ozawa, S. Ogawa, T. Matsuyama, The 150-kilodalton oxygen-regulated protein ameliorates lipopolysaccharide-induced acute lung injury in mice, Am. J. Pathol. 165 (2004) 1279–1288.
[16] W.E. Lawson, P.F. Crossno, V.V. Polosukhin, J. Roldan, D.S. Cheng, K.B. Lane, T.R. Blackwell, C. Xu, C. Markin, L.B. Ware, G.G. Miller, J.E. Loyd, T.S. Blackwell, Endoplasmic reticulum stress in alveolar epithelial cells is prominent in IPF: association with altered surfactant protein processing and herpesvirus infection, Am. J. Physiol. Lung Cell. Mol. Physiol. 294 (2008) L1119–L1126.
[17] M. Korfei, C. Ruppert, P. Mahavadi, I. Henneke, P. Markart, M. Koch, G. Lang, L. Fink, R.M. Bohle, W. Seeger, T.E. Weaver, A. Guenther, Epithelial endoplasmic reticulum stress and apoptosis in sporadic idiopathic pulmonary fibrosis, Am. J. Respir. Crit. Care Med. 178 (2008) 838–846.
[18] H.A. Baek, D.S. Kim, H.S. Park, K.Y. Jang, M.J. Kang, D.G. Lee, W.S. Moon, H.J. Chae, M.J. Chung, Involvement of endoplasmic reticulum stress in myofibroblastic differentiation of lung fibroblasts, Am. J. Respir. Cell Mol. Biol. (2011).
[19] L.M. Nogee, A.E. Dunbar 3rd, S.E. Wert, F. Askin, A. Hamvas, J.A. Whitsett, A mutation in the surfactant protein C gene associated with familial interstitial lung disease, N. Engl. J. Med. 344 (2001) 573–579.
[20] A.Q. Thomas, K. Lane, J. Phillips 3rd, M. Prince, C. Markin, M. Speer, D.A. Schwartz, R. Gaddipati, A. Marney, J. Johnson, R. Roberts, J. Haines, M. Stahlman, J.E. Loyd, Heterozygosity for a surfactant protein C gene mutation associated with usual interstitial pneumonitis and cellular nonspecific interstitial pneumonitis in one kindred, Am. J. Respir. Crit. Care Med. 165 (2002) 1322–1328.
[21] S. Mulugeta, V. Nguyen, S.J. Russo, M. Muniswamy, M.F. Beers, A surfactant protein C precursor protein BRICHOS domain mutation causes endoplasmic reticulum stress, proteasome dysfunction, and caspase 3 activation, Am. J. Respir. Cell Mol. Biol. 32 (2005) 521–530.
[22] H. Tanjore, D.S. Cheng, A.L. Degryse, D.F. Zoz, R. Abdolrasulnia, W.E. Lawson, T.S. Blackwell, Alveolar epithelial cells undergo epithelial-to-mesenchymal transition in response to endoplasmic reticulum stress, J. Biol. Chem. 286 (2011) 30972–30980.
[23] M. Matsuda, T. Hoshino, Y. Yamashita, K. Tanaka, D. Maji, K. Sato, H. Adachi, G. Sobue, H. Ihn, Y. Funasaka, T. Mizushima, Prevention of UVB radiation-induced epidermal damage by expression of heat shock protein 70, J. Biol. Chem. 285 (2010) 5848–5858.
[24] K. Tanaka, K. Sato, K. Aoshiba, A. Azuma, T. Mizushima, Superiority of PC-SOD to other anti-COPD drugs for elastase-induced emphysema and alteration in lung mechanics and respiratory function in mice, Am. J. Physiol. Lung Cell. Mol. Physiol. 302 (2012) L1250–L1261.
[25] K. Tanaka, T. Ishihara, A. Azuma, S. Kudoh, M. Ebina, T. Nukiwa, Y. Sugiyama, Y. Tasaka, T. Namba, K. Sato, Y. Mizushima, T. Mizushima, Therapeutic effect of lecithinized superoxide dismutase on bleomycin-induced pulmonary fibrosis, Am. J. Physiol. Lung Cell. Mol. Physiol. 298 (2010) L348–L360.
[26] K. Tanaka, Y. Tanaka, T. Namba, A. Azuma, T. Mizushima, Heat shock protein 70 protects against bleomycin-induced pulmonary fibrosis in mice, Biochem. Pharmacol. 80 (2010) 920–931.
[27] S. Mima, S. Tsutsumi, H. Ushijima, M. Takeda, I. Fukuda, K. Yokomizo, K. Suzuki, K. Sano, T. Nakanishi, W. Tomisato, T. Tsuchiya, T. Mizushima, Induction of claudin-4 by nonsteroidal anti-inflammatory drugs and its contribution to their chemopreventive effect, Cancer Res. 65 (2005) 1868–1876.
[28] T. Namba, T. Hoshino, K. Tanaka, S. Tsutsumi, T. Ishihara, S. Mima, K. Suzuki, S. Ogawa, T. Mizushima, Up-regulation of 150-kDa oxygen-regulated protein by celecoxib in human gastric carcinoma cells, Mol. Pharmacol. 71 (2007) 860–870.
[29] K. Ask, R. Labiris, L. Farkas, A. Moeller, A. Froese, T. Farncombe, G.B. McClelland, M. Inman, J. Gauldie, M.R. Kolb, Comparison between conventional and "clinical" assessment of experimental lung fibrosis, J. Transl. Med. 6 (2008) 16.

See related commentary on pg 868

ORIGINAL ARTICLE

# Suppression of UV-Induced Wrinkle Formation by Induction of HSP70 Expression in Mice

Minoru Matsuda[1,2,3], Tatsuya Hoshino[1], Naoki Yamakawa[1,2], Kayoko Tahara[1], Hiroaki Adachi[4], Gen Sobue[4], Daisuke Maji[3], Hironobu Ihn[2] and Tohru Mizushima[1]

UV-induced wrinkle formation owing to the degeneration of the extracellular matrix (ECM) is a major dermatological problem in which abnormal activation of matrix metalloproteinases (MMPs) and elastases have important roles. Heat shock protein 70 (HSP70) has cytoprotective and anti-inflammatory activities. In this study, we examined the effect of HSP70 expression on UV-induced wrinkle formation. Mild heat treatment (exposure to heated water at 42 °C) of the dorsal skin of hairless mice induced the expression of HSP70. The long-term repeated exposure to UV induced epidermal hyperplasia, decreased skin elasticity, degeneration of ECM, and wrinkle formation, which could be suppressed in mice concomitantly subjected to this heat treatment. The UV-induced epidermal hyperplasia, decreased skin elasticity, and degeneration of ECM were less apparent in transgenic mice expressing HSP70 than in wild-type mice. UV-induced fibroblast cell death, infiltration of inflammatory cells, and activation of MMPs and elastase in the skin were also suppressed in the transgenic mice. This study provides evidence for an inhibitory effect of HSP70 on UV-induced wrinkle formation. The results suggest that this effect is mediated by various properties of HSP70, including its cytoprotective and anti-inflammatory activities. We propose that HSP70 inducers used in a clinical context could prove beneficial for the prevention of UV-induced wrinkle formation.

*Journal of Investigative Dermatology* (2013) **133,** 919–928; doi:10.1038/jid.2012.383; published online 25 October 2012

## INTRODUCTION

The skin is damaged by various environmental stressors, especially by long-term chronic solar UV radiation (photoaging). UV light can be separated according to wavelength, with UVB thought to have an important role in photoaging (Matsumura and Ananthaswamy, 2004; Rabe *et al.*, 2006). This process is mediated not only by direct UV-induced damage to the skin but also indirectly via the induction of inflammation and production of reactive oxygen species that are released from infiltrated leukocytes (Rabe *et al.*, 2006).

Both wrinkle formation and skin hyperpigmentation disorders are major dermatological problems. It is believed that epidermal hyperplasia owing to epidermal damage and inflammation, as well as alteration of the extracellular matrix (ECM) (such as damage to collagen fibers, suppression of collagen expression, disruption and degeneration of elastic fibers, and disruption of the epidermal basal membrane), has an important role in UV-induced wrinkle formation and decreased skin elasticity, which is closely linked to wrinkle formation (Talwar *et al.*, 1995; Imokawa, 2009; Rijken and Bruijnzeel, 2009). As these UV-induced phenomena can be reproduced to some extent in hairless mice exposed to long-term repeated exposure to UVB radiation, this animal model has been used to examine the mechanism of UV-induced wrinkle formation (Schwartz, 1988).

Matrix metalloproteinases (MMPs)-dependent qualitative and quantitative decreases in the ECM have an important role in UV-induced wrinkle formation. The activities of MMP-1, 2, 3, and 9 were increased by UVB irradiation in mouse and human skin (Inomata *et al.*, 2003; Rabe *et al.*, 2006), whereas the topical treatment of mouse skin with MMP inhibitors blocked UV-induced wrinkle formation, and decreased skin elasticity and basal membrane disruption (Inomata *et al.*, 2003). In mouse, MMP-2, 8, and 13, or MMP-2 and 9, are responsible for the degradation of collagen types I or IV, respectively, which constitute dermal collagen fibers or the epidermal basal membrane, respectively (Aimes and Quigley, 1995; Visse and Nagase, 2003; Kessenbrock *et al.*, 2010). In addition to collagenases (MMP-8 and 13), gelatinases (MMP-2 and 9) have important roles in UV-induced wrinkle formation, decreased skin elasticity, and basal membrane disruption (Inomata *et al.*, 2003). Tissue inhibitors of MMPs (TIMPs) also have important roles in these phenomena. The disruption

[1]*Department of Analytical Chemistry, Faculty of Pharmacy, Keio University, Tokyo, Japan;* [2]*Graduate School of Medical and Pharmaceutical Sciences, Kumamoto University, Kumamoto, Japan;* [3]*Saishunkan Pharmaceutical, Kumamoto, Japan and* [4]*Nagoya University Graduate School of Medicine, Nagoya, Japan*

*Correspondence: Tohru Mizushima, Department of Analytical Chemistry, Faculty of Pharmacy, Keio University, Tokyo 105-8512, Japan. E-mail: mizushima-th@pha.keio.ac.jp*

*Abbreviations: ECM, extracellular matrix; HSPs, heat shock proteins; MMPs, matrix metalloproteinases; TIMPs, tissue inhibitors of MMPs*

*Received 30 November 2011; revised 23 July 2012; accepted 6 August 2012; published online 25 October 2012*

and degeneration of elastic fibers also have an important role in wrinkle formation and decreased skin elasticity (Imokawa, 2009). To this extent, the topical application of elastase inhibitors significantly suppressed UV-induced wrinkle formation in hairless mice (Tsuji *et al.*, 2001; Tsukahara *et al.*, 2001; Zhao *et al.*, 2009).

Induction of the expression of heat shock proteins (HSPs), especially that of HSP70, provides resistance to stressors (Morimoto and Santoro, 1998). In addition to this cytoprotective effect, HSP70 has an anti-inflammatory activity (Krappmann *et al.*, 2004; Chen *et al.*, 2006; Tang *et al.*, 2007; Weiss *et al.*, 2007). The artificial expression of HSP70 in keratinocytes and melanocytes confers protection *in vitro* against UV (Maytin *et al.*, 1994; Trautinger *et al.*, 1995; Park *et al.*, 2000; Wilson *et al.*, 2000; Trautinger, 2001). However, the role of HSP70 in photoaging *in vivo* remains unclear. We recently showed that UV-induced skin damage and the resulting inflammatory responses were suppressed in transgenic mice expressing HSP70 (Matsuda *et al.*, 2010). We also reported that UV-induced melanin production by the skin was suppressed in transgenic mice expressing HSP70 (Hoshino *et al.*, 2010). However, the role of HSP70 in UV-induced wrinkle formation is yet to be elucidated.

In this study, we examine the effect of the expression of HSP70 on UV-induced wrinkle formation and decreased skin elasticity. UV-induced epidermal hyperplasia, decreased skin elasticity, and wrinkle formation were suppressed in hairless mice concomitantly subjected to mild heat treatment (exposure to heated water at 42 °C). Moreover, UV-induced epidermal hyperplasia, decreased skin elasticity, the disruption of collagen and elastic fibers, and the basal membrane of the epidermis, and activation of MMPs and elastase were significantly suppressed in transgenic mice expressing HSP70 compared with wild-type mice. These results suggest that HSP70 expression protects the skin against UV-induced wrinkle formation.

## RESULTS

### Effect of heat treatment on UVB-induced wrinkle formation

We examined the effect of a single mild heat treatment (exposure to heated water, 42 °C for 5 minutes) on HSP expression in the dorsal skin of hairless mice. Immunoblotting analysis revealed that the level of HSP70 but not of other HSPs in the skin increased after the heat treatment (Figure 1a and b). The induction of expression of HSP70 by the mild heat treatment (42 °C for 5 minutes) was observed even after the repeated heat treatment (three times a week for 5 weeks) (Figure 1c and d). Costaining of HSP70 and pan-cytokeratin (a keratinocyte marker), vimentin (a fibroblast marker), or CD11b (a macrophage marker) was observed in both repeatedly heat-treated and untreated dorsal skin (Figure 1e–g). We confirmed mild heat treatment–induced expression of HSP70 in mice irradiated with UVB (Figure 1c–g).

To examine the effect of expression of HSPs on UVB-induced wrinkle formation, the dorsal skin of animals was pre-exposed to the heat treatment (exposure to heated water, 42 °C for 5 minutes) and then irradiated with UVB. This cycle was repeated three times a week for 10 weeks. As shown in Figure 2a and b, visible signs of wrinkling were observed in the dorsal skin of UVB-treated control mice (without heat treatment), but not so clearly in that of mice treated with both UVB and heat. The area of shadow on the replica images, which is indicative of wrinkle formation level, was increased by exposure to UVB radiation, whereas concomitant heat treatment reduced this index in UVB-treated mice (Figure 2c and d). These results suggest that the heat treatment suppresses UVB-induced wrinkle formation.

We then used a Cutometer to examine the effect of heat treatment on UVB-induced alterations to skin elasticity. All indexes of skin elasticity (Uf, final distension; Ue, immediate distension; and Ur, immediate retraction) except for Uv (delayed distension) were decreased by the UVB radiation and were significantly higher in heat-treated skin than in untreated skin exposed to UVB radiation (Figure 2e), suggesting that heat treatment suppresses the UVB-induced decrease in skin elasticity.

Epidermal hyperplasia is also closely linked to wrinkle formation. The UVB irradiation induced epidermal hyperplasia, although the epidermal thickness was lower in mice subjected to concomitant heat treatment than in control mice exposed to UVB radiation (Figure 2f and g).

We then used immunohistochemical analysis to examine the effect of the heat treatment on the ECM. As shown in Figure 3a, the layer expressing type IV collagen (the epidermal basal membrane) was disrupted in UVB-treated control mice (without heat treatment). This effect, however, was attenuated in mice concomitantly exposed to heat treatment.

Total expression of type I collagen and fine collagen fibers was decreased in UVB-exposed control mice (without heat treatment), and these decreases were suppressed in mice that had been concomitantly exposed to heat treatment (Figure 3a). Similar results were observed for elastic fibers, which were identified by the immunohistochemical detection of tropoelastin (Figure 3a). The results in Figure 3a suggest that heat treatment suppressed the UVB-induced disruption and degeneration of the skin's ECM.

### UVB-induced wrinkle formation–related phenomena in transgenic mice expressing HSP70

We then compared the UVB-induced decrease in skin elasticity and epidermal hyperplasia between transgenic mice expressing HSP70 (Plumier *et al.*, 1995) and wild-type mice. UVB-induced decreased skin elasticity (decrease in Uf, Ue, and Ur indexes) was observed in wild-type mice; these indexes were significantly higher in UVB-treated transgenic mice expressing HSP70 (Figure 4a). Similar results were observed for epidermal hyperplasia; the epidermal thickness was lower in transgenic mice than in wild-type mice after UVB irradiation (Figure 4b and c). These results show that the UVB-induced decrease in skin elasticity and epidermal hyperplasia observed in wild-type mice was suppressed in transgenic mice expressing HSP70.

The UVB-induced degradation of the epidermal basal membrane and the decrease in collagen and elastic fibers were not observed as clearly in transgenic mice expressing HSP70 as they were in wild-type mice (Figure 3b).

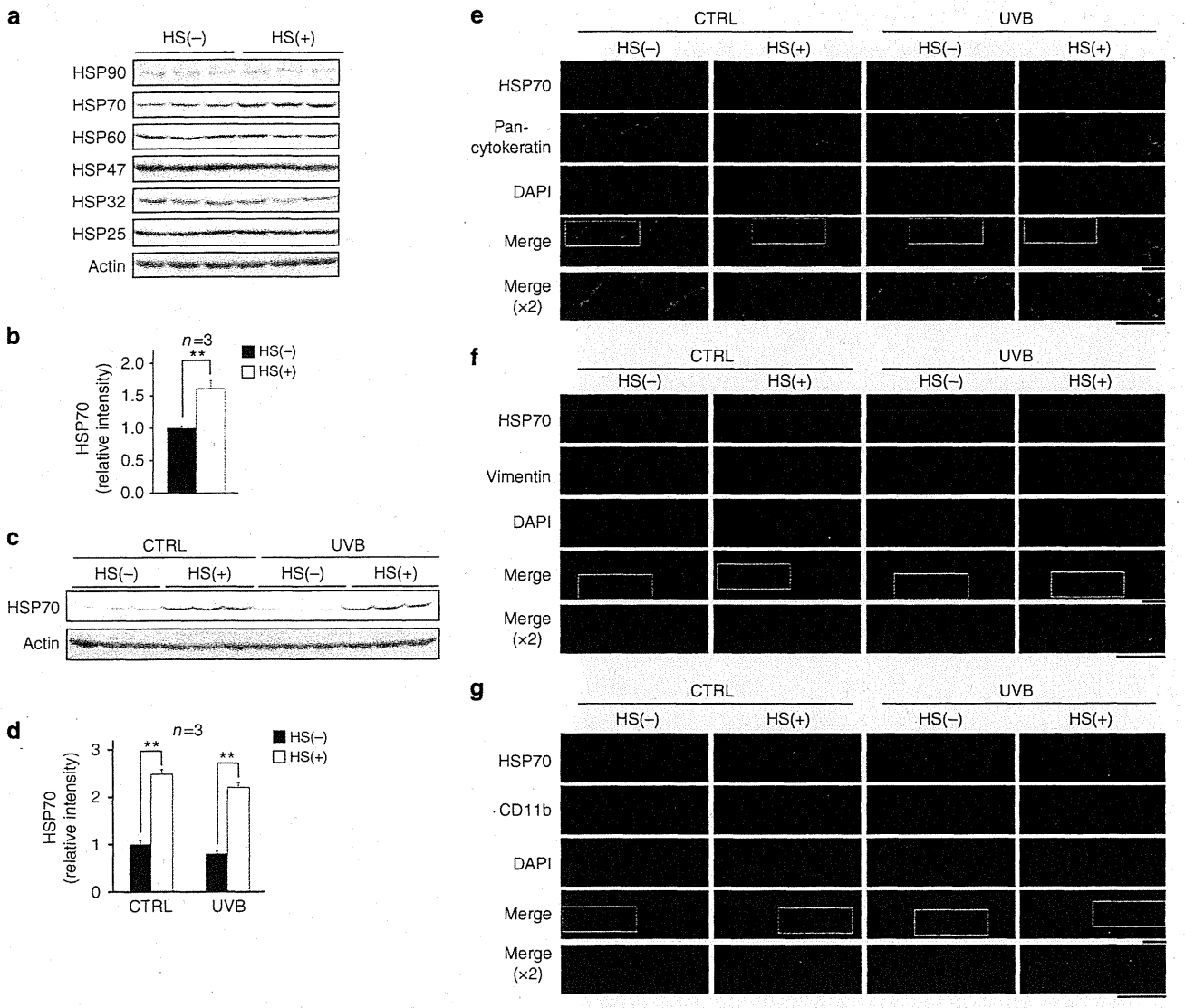


**Figure 1. Expression of heat shock proteins (HSPs) in the dorsal skin after heat treatment.** (**a**, **b**) The dorsal skin of hairless mice was exposed to heated water at 42 °C (HS(+)) or 37 °C (HS(−)) for 5 minutes. (**c**–**g**) Six hours after this heat treatment, mice were irradiated with UVB. This cycle was repeated three times a week for 5 weeks. (**a**–**g**) Dorsal skin was removed 6 hours after the final heat treatment. (**a**, **c**) Samples were analyzed by immunoblotting with antibodies against each protein. (**b**, **d**) The band intensity was determined. Values are mean ± SEM. $^{**}P<0.01$. (**e**–**g**) Sections were subjected to immunohistochemical analysis with antibodies against HSP70 and pan-cytokeratin (**e**), vimentin (**f**), or CD11b (**g**). Bar = 50 μm. CTRL, control; DAPI, 4,6-diamidino-2-phenylindole dihydrochloride.

### Mechanism for the protective role of HSP70 against UVB-induced wrinkle formation–related phenomena

We then determined by TUNEL assay the extent of UVB-induced fibroblast cell death. An increase in the number of TUNEL-positive cells in the skin of wild-type mice was observed after a single UVB irradiation, and this increase was clearly suppressed in transgenic mice expressing HSP70 (Figure 5a). Immunostaining for vimentin was also performed, and the number of cells positive for both TUNEL and vimentin staining was counted. The number of double-positive cells increased in response to UVB irradiation in wild-type mice, and this number was lower in transgenic mice expressing HSP70 (Figure 5b), suggesting that HSP70 expression protected skin fibroblasts from UVB-induced cell death.

To test this idea *in vitro*, we prepared primary cultures of skin fibroblasts from the transgenic and wild-type mice and examined the level of resistance of these cells to hydrogen peroxide. As shown in Figure 5c, treatment of wild-type skin fibroblasts with hydrogen peroxide decreased cell viability; this decrease was significantly suppressed in HSP70-over-expressing skin fibroblasts, showing that the expression of HSP70 protected the skin fibroblasts against reactive oxygen species-induced cell death.

Next, we examined the mechanism for the protective effect of HSP70 against UVB-induced alterations to the ECM. As messenger RNA expression levels corresponding to proα1(I)-collagen, proα2(I)collagen, proα1(IV)collagen, proα2(IV)collagen, and tropoelastin were indistinguishable between transgenic

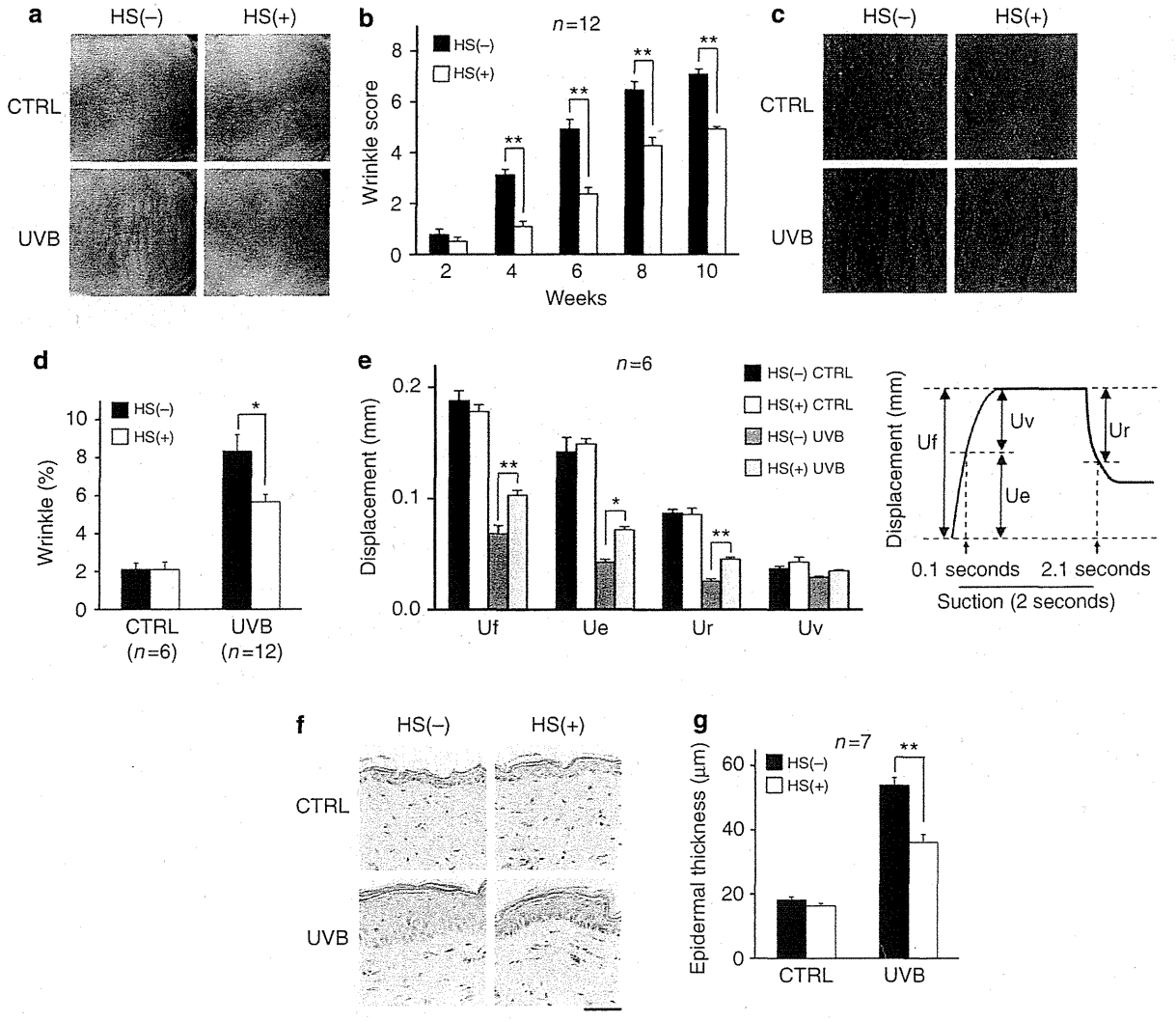


**Figure 2. Effect of heat treatment on UVB-induced wrinkle formation.** Heat treatment of the dorsal skin was performed, and 6 hours later mice were irradiated with UVB. This cycle was repeated three times a week for 10 weeks. (**a**) Typical photographs of the dorsal skin. (**b**) The wrinkle score was determined. (**c**) Typical replica images of the skin are shown. (**d**) The relative area of wrinkles was calculated. (**e**) Skin elasticity was measured by a Cutometer. The standard time-course profile was shown. (**f–g**) The dorsal skin was removed 24 hours after the final UVB irradiation and sections were subjected to histological examination (**f**). The epidermal thickness was measured (**g**). Values are mean ± SEM. $^{**}P<0.01$; $^{*}P<0.05$. CTRL, control.

mice expressing HSP70 and wild-type mice under conditions both with and without UVB irradiation (data not shown), we then focused on MMPs and elastase. We used gelatin zymography to examine the activities of MMP-2 and MMP-9. The band intensities of MMP-2 and MMP-9, indicative of MMP-2 and MMP-9 activities, were higher in skin tissues prepared from UVB-treated wild-type mice than in those from UVB-treated transgenic mice expressing HSP70 (Figure 6a and b). Similar results were obtained for elastase activity (Figure 6c). On the other hand, the type I collagenase or MMP-13 activity was indistinguishable between the transgenic mice and wild-type mice (Figure 6d and e). The amount of MMP-13 or TIMP-1 in dorsal skin extract was also indistinguishable between them (data not shown). These results suggest that the expression of HSP70 suppresses the UVB-induced activation of MMP-2, MMP-9, and elastase.

To test this idea *in vitro*, we compared the activities of these proteases in primary cultures of skin fibroblasts. The MMP-2 activity was higher in wild-type fibroblasts than in HSP70-expressing fibroblasts in both the presence and absence of hydrogen peroxide (Figure 6f and g). We could not detect MMP-9 activity (Figure 6f). The messenger RNA expression level corresponding to MMP-2 was higher in wild-type fibroblasts than in HSP70-expressing cells (Figure 6h). As for elastase, although the activity in the absence of hydrogen peroxide was indistinguishable between wild-type and HSP70-expressing fibroblasts, the activity was higher in wild-type fibroblasts than in HSP70-expressing fibroblasts in the presence of hydrogen peroxide (Figure 6i). We could not detect messenger RNA expression corresponding to elastase under the conditions used (data not shown). These results support the idea that the expression of HSP70 suppresses MMP-2 and elastase activities.

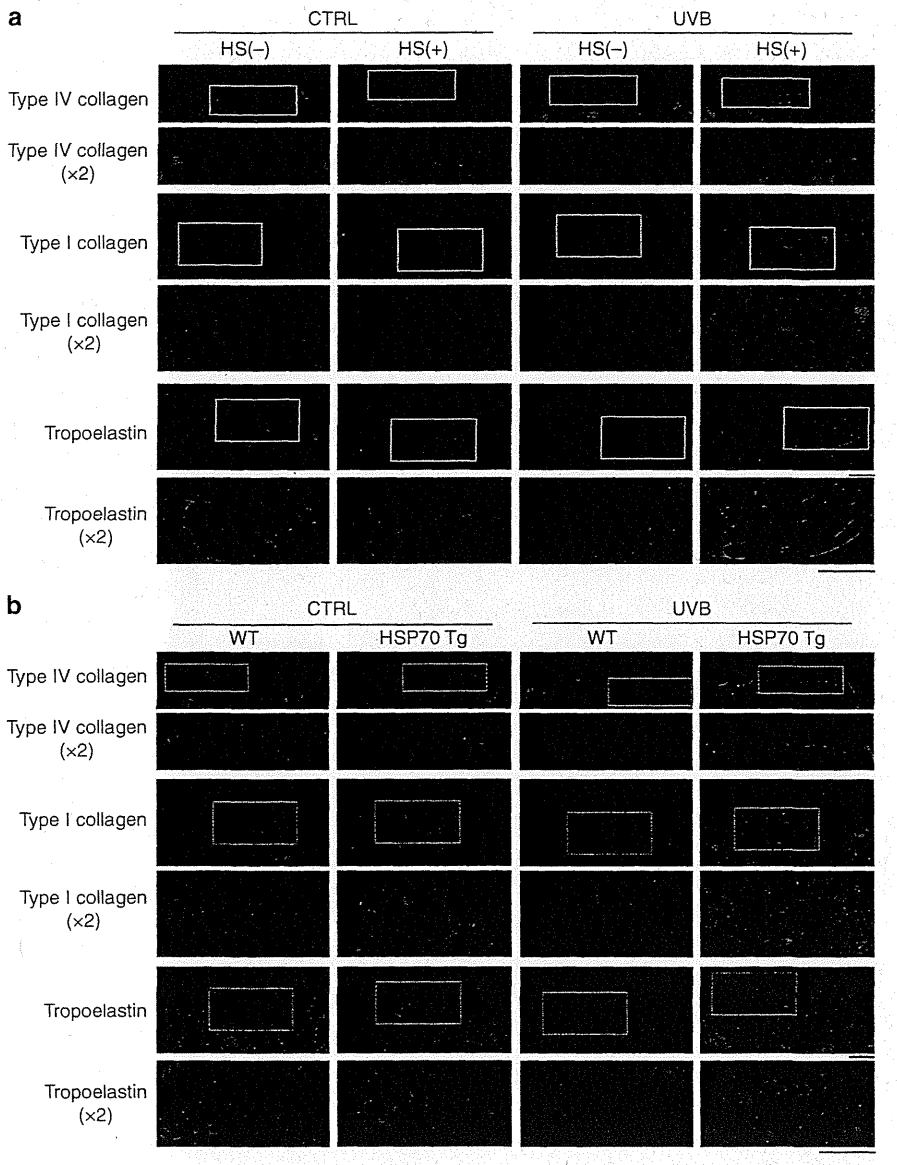


**Figure 3. Effect of heat shock protein 70 (HSP70) expression on UVB-induced alteration of extracellular matrix.** (**a**) Heat treatment and UVB irradiation of the dorsal skin of hairless mice were performed as described in the legends of Figure 2. (**b**) Transgenic mice expressing HSP70 (HSP70 Tg) and wild-type mice (WT) were irradiated with UVB three times a week for 6 weeks. (**a**, **b**) The dorsal skin was removed 24 hours after the final UVB irradiation and subjected to immunohistochemical analysis with antibodies against type IV collagen, type I collagen, or tropoelastin. Bar = 50 μm. CTRL, control.

In relation to MMP-9, it was reported that inflammatory cells such as macrophages and neutrophils produce this protein (Kessenbrock *et al.*, 2010). We therefore used immunohistochemical analysis to examine the infiltration of these cells in the skin of UVB-treated or untreated transgenic mice expressing HSP70 or their wild-type counterparts. As shown in Figure 6j, the number of CD11b-positive cells (macrophages) or myeloperoxidase-positive cells (neutrophils) in the skin was increased by UVB irradiation in wild-type mice. This number was lower in UVB-treated transgenic mice expressing HSP70, suggesting that the expression of HSP70 inhibits the UVB-induced infiltration of macrophages and neutrophils into the skin. We also used gelatin zymography to compare the activities of MMPs in HSP70-overexpressing and wild-type macrophages, and found that the MMP-9 activity was similar between the two types of macrophages (data not shown). These results suggest that the expression of HSP70 suppresses MMP-9 activity by inhibiting the UVB-induced infiltration of macrophages and neutrophils into the skin.

## DISCUSSION

Here we provide data suggesting that HSP70 is protective against UVB-induced wrinkle formation.

UVB-induced wrinkle formation requires a long period of irradiation (about 10 weeks). Thus, it is difficult to monitor UVB-induced wrinkle formation in normal mice (with hair) because a true hairless state with shaved skin can only be maintained for about 6–7 weeks. For this reason, hairless mice

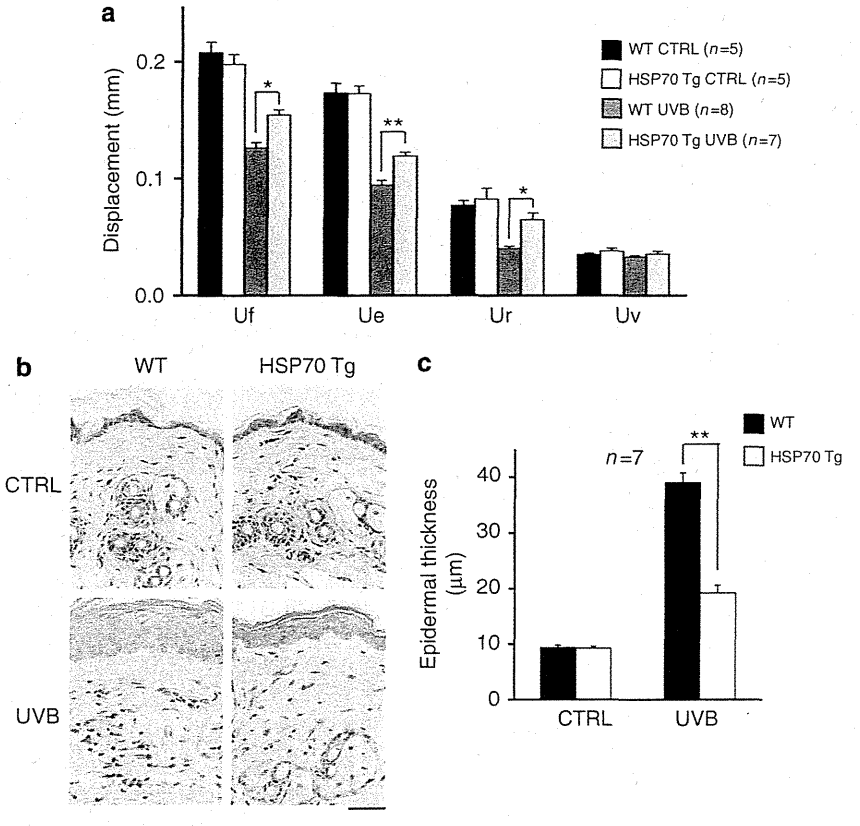


**Figure 4. UVB-induced decrease in skin elasticity and epidermal hyperplasia in transgenic mice expressing heat shock protein 70 (HSP70).** Transgenic mice expressing HSP70 (HSP70 Tg) and wild-type mice (WT) were irradiated with UVB as described in the legend of Figure 3. The skin elasticity (**a**) and epidermal thickness (**b**, **c**) were measured and shown as described in the legend of Figure 2. Values are mean ± SEM. $^{**}P<0.01$; $^{*}P<0.05$. CTRL, control.

were used in the study to examine the wrinkle formation. On the other hand, transgenic mice are useful to examine the role of specific proteins in biological responses. For this reason, we studied the role of HSPs on wrinkle formation using heat treatment of hairless mice, whereas the mechanism for the protective role of HSP70 on wrinkle formation was examined in transgenic mice expressing HSP70.

It was previously reported that more severe heat treatment conditions (e.g., 43 °C for 30 or 90 minutes) than those in this study (42 °C for 5 minutes) causes skin damage such as wrinkle formation and activation of MMPs *in vivo* (Cho *et al.*, 2008, 2009; ; Kim *et al.*, 2009; Shin *et al.*, 2012). We confirmed that heat treatment of mouse skin under severe conditions (43, 44, or 45 °C for 5 minutes) but not under mild conditions (42 °C for 5 minutes) caused an increase in the amount of MMP-13 (data not shown). We also observed an increase in the amounts and/or activities of MMP-2, MMP-9, and elastase in mouse skin by heat treatment of severe conditions (data not shown). On the other hand, we found that treatment of mouse skin at 42 °C or higher for 5 minutes clearly induced the expression of HSP70 (Figure 1 and data not shown). As the purpose of this study is to examine the protective role of HSP70 induced by heat treatment on the UVB-induced wrinkle formation, we used the mild heat treatment conditions (42 °C for 5 minutes). However, it should be noted that severe heat treatment damages the skin even without concomitant exposure to UVB.

We found that mild heat treatment of the dorsal skin of hairless mice suppressed UVB-induced wrinkle formation, and decrease in skin elasticity and epidermal hyperplasia. This is an evidence showing that mild heat treatment protects against UVB-induced wrinkle formation. Furthermore, the UVB-induced decrease in skin elasticity and epidermal hyperplasia was less apparent in transgenic mice expressing HSP70 compared with wild-type mice, suggesting that the mild heat treatment suppresses UVB-induced wrinkle formation through the induction of HSP70 expression.

UVB-induced wrinkle formation is mediated by a complex mechanism involving damage to the ECM and cell death, and the resulting inflammatory responses both in the epidermis and dermis. We showed here that exposure to UVB radiation caused skin fibroblast cell death and that this was suppressed in transgenic mice expressing HSP70. We also showed that reactive oxygen species-induced cell death was suppressed in HSP70-overexpressing skin fibroblasts compared with control fibroblasts cultured *in vitro*. Similar results were observed for keratinocytes in our previous paper (Matsuda *et al.*, 2010). We also found that compared with wild-type mice, the infiltration of inflammatory cells (macrophages and neutrophils) after long-term repeated UVB irradiation of animals was suppressed in transgenic mice expressing HSP70. We previously reported that a single UVB irradiation of wild-type mice decreased the skin level of IκB-α (an inhibitor of NF-κB) and increased proinflammatory cytokines and chemokines in the

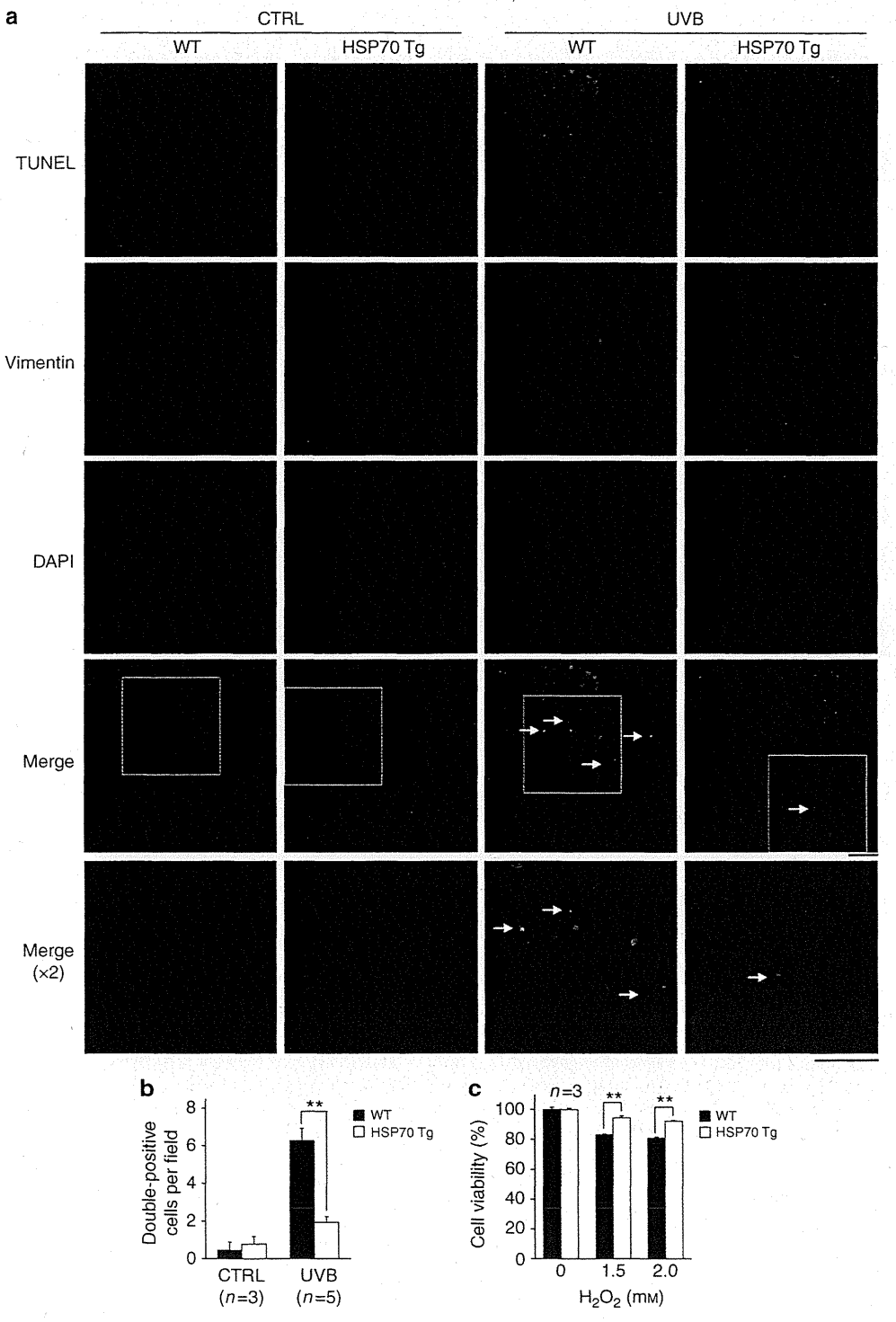


**Figure 5. UVB-induced fibroblast cell death in transgenic mice expressing heat shock protein 70 (HSP70).** (**a**, **b**) Transgenic mice expressing HSP70 (HSP70 Tg) and wild-type mice (WT) were irradiated with 180 mJ cm$^{-2}$ UVB, and the dorsal skin was removed after 24 hours. (**a**) Sections were subjected to TUNEL assay, immunohistochemical analysis with antibody against vimentin, and 4,6-diamidino-2-phenylindole dihydrochloride (DAPI) staining (double-positive cells are shown by arrows; bar = 50 μm). (**b**) The number of double-positive cells (TUNEL and vimentin expression) was counted. (**c**) Primary cultures of skin fibroblasts prepared from HSP70 Tg and WT were treated with the indicated concentrations of hydrogen peroxide for 1 hour and cultured for 23 hours. Cell viability was determined by the 3-(4,5-dimethylthiazol-2-yl)-2,5-diphenyl tetrazolium bromide method. Values are mean ± SEM. $^{**}P<0.01$. CTRL, control.

skin, and that these inflammatory responses were suppressed in transgenic mice expressing HSP70 (Matsuda *et al.*, 2010). Taken together, these results suggest that the cytoprotective and anti-inflammatory activities of HSP70 contribute to the suppression of UVB-induced phenomena related to wrinkle formation (decrease in skin elasticity and epidermal

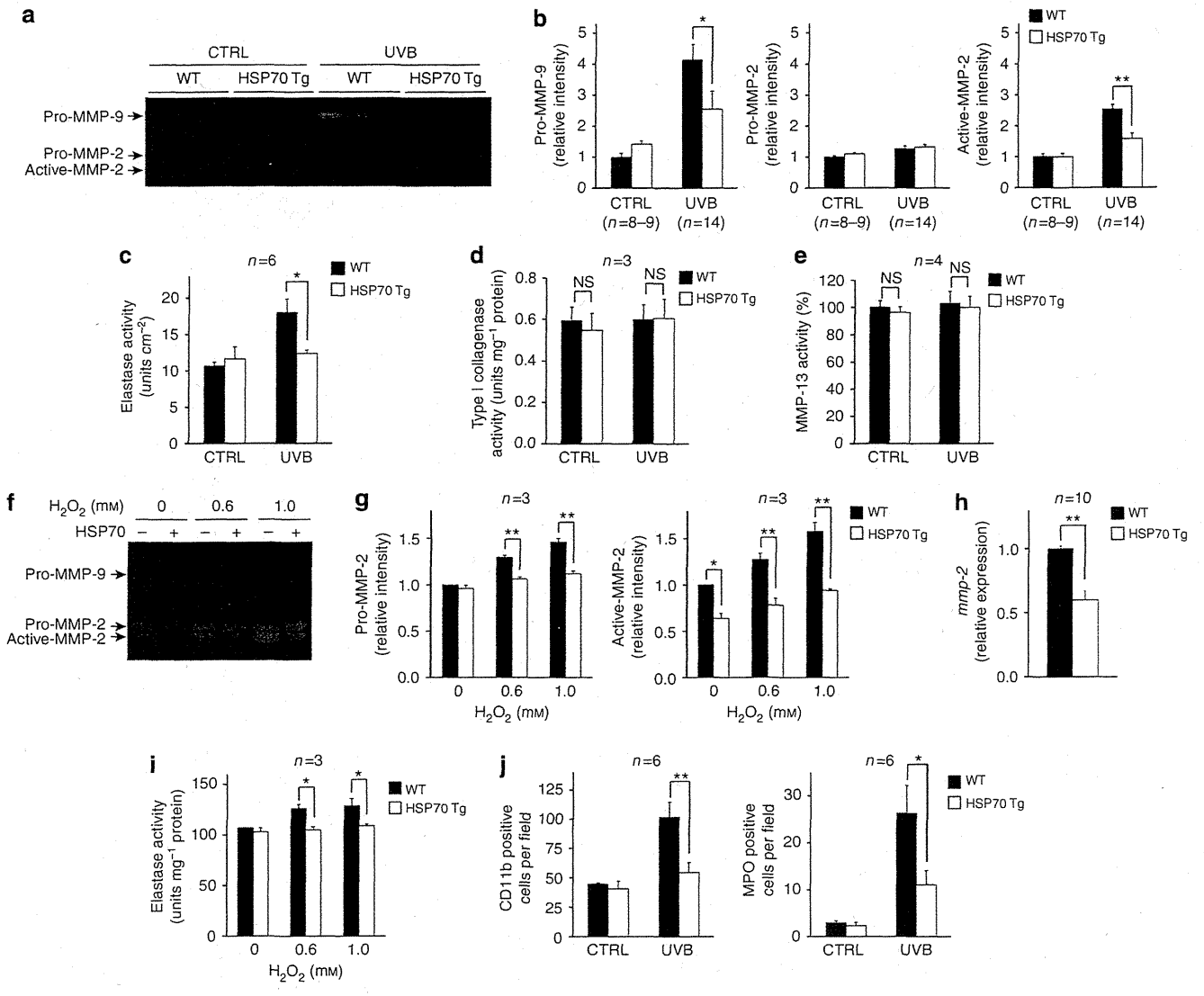


**Figure 6. Effect of heat shock protein 70 (HSP70) overexpression on matrix metalloproteinases (MMPs) and elastase activities.** (**a–e**, **j**) Mice were irradiated with UVB as described in the legend of Figure 3. (**f–i**) Primary skin fibroblasts were treated with hydrogen peroxide as described in the legend of Figure 5. Dorsal skin extracts (**a**) or culture media (**f**) were subjected to gelatin zymography assay, and the band intensity was determined (**b**, **g**). Elastase (**c**), type I collagenase (**d**), or MMP-13 (**e**) activity in dorsal skin extracts or elastase activity in cells (**i**) was measured. The messenger RNA expression was analyzed (**h**). The dorsal skin was subjected to immunohistochemical analysis for CD11b or myeloperoxidase, and the number of positive cells was counted (**j**). Values are mean ± SEM. $^{**}P<0.01$; $^{*}P<0.05$. CTRL, control; NS, not significant; WT, wild type.

hyperplasia) in transgenic mice expressing HSP70 and wild-type mice exposed to heat treatment.

Immunohistochemical analysis suggested that the level of type I collagen was decreased by UVB irradiation in control mice and that this decrease was partially suppressed in mice concomitantly exposed to mild heat treatment, or in transgenic mice expressing HSP70. This analysis also showed that fine basal membrane of the epidermis and collagen and elastic fibers were disrupted by UVB irradiation; this damage was partially suppressed in mice concomitantly exposed to mild heat treatment or in transgenic mice expressing HSP70. We also found that the activities of MMP-2, MMP-9, and elastase were increased by UVB irradiation and that these activities were lower in UVB-treated transgenic mice expressing HSP70 than in wild-type mice. These results suggest that MMP-2, MMP-9, and elastase have important roles in the HSP70-dependent protection against UVB-induced disruption of the ECM. As the overexpression of HSP70 in primary cultures of skin fibroblasts suppressed the expression and activity of MMP-2 and the activity of elastase, HSP70 seems to directly suppress the expression and/or activity of these proteases. On the other hand, the expression of HSP70 did not affect the activity of MMP-9 in macrophage primary cultures, suggesting that the decreased MMP-9 activity in UVB-treated transgenic mice expressing HSP70 may be owing to the suppression of infiltration of inflammatory cells into the skin.

We recently found that the artificial expression of HSP70 suppresses melanin production both *in vivo* and *in vitro* (Hoshino *et al.*, 2010). We also reported that HSP70 expression suppresses both UVB-induced cellular and DNA damage

and production of reactive oxygen species (Matsuda *et al.*, 2010). As UV-induced modest melanin production has an important role in protecting the skin against UV-dependent damage (Kobayashi *et al.*, 1998), our results suggest that HSP70 inducers could serve as hypopigmenting agents (skin whitening agents) without worsening UV-induced skin damage. The results of this study suggest that such HSP70 inducers could also be beneficial for reducing UV-induced wrinkle formation.

## MATERIALS AND METHODS

### Animals

The experiments and procedures described here were performed in accordance with the Guide for the Care and Use of Laboratory Animals as adopted and promulgated by the National Institutes of Health, and were approved by the Animal Care Committee of Kumamoto University and Keio University.

### UVB irradiation and heat treatment

Animals were exposed to UVB radiation with a double bank of UVB lamps (peak emission at 312 nm, VL-215LM lamp, Vilber Lourmat, Paris, France). This UV lamp mainly emits UVB but emits a small level of UVA. Animals were placed under deep anesthesia with chloral hydrate (250 mg $kg^{-1}$), and the fur (except in the case of hairless mice) was removed with electric clippers before the first UVB irradiation.

The dorsal skin of hairless mice was exposed to heated water at 42 °C or 37 °C (control) for 5 minutes for heat treatment.

Wrinkles were formed as a consequence of long-term, repeated exposure to UVB radiation (three times a week for 6 or 10 weeks) as described previously (Inomata *et al.*, 2003) with some modifications. Briefly, in the case of hairless mice, the initial dose of UVB was set at 36 mJ $cm^{-2}$, which was subsequently increased weekly to 54, 72, 90, 108, 126, 144, 162, and finally 180 mJ $cm^{-2}$ (180 mJ $cm^{-2}$, both at week 9 and week 10; a total of 10 weeks). In the case of transgenic mice expressing HSP70 and the wild-type mice (C57/BL6), the initial dose was set at 36 mJ $cm^{-2}$, which was subsequently increased weekly to 54, 72, 108, 144, and 180 mJ $cm^{-2}$ (a total of 6 weeks).

### Wrinkle scoring, image analysis of skin replicas, and measurement of skin elasticity

Evaluation of wrinkle formation was performed by both visual wrinkle scoring and image analysis of skin replicas as described previously (Inomata *et al.*, 2003; Tsukahara *et al.*, 2004). Skin elasticity was measured with a Cutometer 575 meter (Courage + Khazaka) as described previously (Agache *et al.*, 1980; Elsner *et al.*, 1990; Tsukahara *et al.*, 2001).

### Real-time reverse-transcriptase–PCR analysis

Total RNA was extracted from cultured cells using the RNeasy Fibrous Tissue Mini kit (Qiagen, Valencia, CA) according to the manufacturer's protocol. Real-time reverse-transcriptase–PCR analysis was performed as described (Hoshino *et al.*, 2010). The primer sequence would be provided on request.

### Histological and immunohistochemical analyses and TUNEL assay

Histological examination (hematoxylin and eosin staining), immunohistochemical analysis, and TUNEL assay were performed as described (Matsuda *et al.*, 2010).

### Gelatin zymography and measurement of enzyme activity

The proteolytic activity of MMP-2 and MMP-9 was assessed by SDS-PAGE using zymogram gels containing 0.1% (w/v) gelatin, as described previously (Taraboletti *et al.*, 2000). Elastase activity was measured using *N*-succinyl-tri-alanyl-p-nitroanilide (Peptide Institute, Osaka, Japan) as a substrate, as described previously (Tsukahara *et al.*, 2004). Type I collagenase activity or MMP-13 activity was measured using the type I collagenase assay kit (Primary Cell, Hokkaido, Japan) or the SensoLyte MMP-13 assay kit (AnaSpec, San Jose, CA), respectively.

### Statistical analysis

All values are expressed as the mean ± SEM. Two-way analysis of variance followed by the Tukey's test was used to evaluate differences between more than two groups. Differences were considered to be significant for values of $P<0.05$.

## CONFLICT OF INTEREST

The authors state no conflict of interest.

## ACKNOWLEDGMENTS

This work was supported by Grants-in-Aid for Scientific Research from the Ministry of Health, Labor, and Welfare of Japan, as well as the Japan Science and Technology Agency and Grants-in-Aid for Scientific Research from the Ministry of Education, Culture, Sports, Science and Technology, Japan.

## REFERENCES

Agache PG, Monneur C, Leveque JL *et al.* (1980) Mechanical properties and Young's modulus of human skin *in vivo*. *Arch Dermatol Res* 269:221–32

Aimes RT, Quigley JP (1995) Matrix metalloproteinase-2 is an interstitial collagenase. Inhibitor-free enzyme catalyzes the cleavage of collagen fibrils and soluble native type I collagen generating the specific 3/4- and 1/4-length fragments. *J Biol Chem* 270:5872–6

Chen H, Wu Y, Zhang Y *et al.* (2006) Hsp70 inhibits lipopolysaccharide-induced NF-kappaB activation by interacting with TRAF6 and inhibiting its ubiquitination. *FEBS Lett* 580:3145–52

Cho S, Lee MJ, Kim MS *et al.* (2008) Infrared plus visible light and heat from natural sunlight participate in the expression of MMPs and type I procollagen as well as infiltration of inflammatory cell in human skin *in vivo*. *J Dermatol Sci* 50:123–33

Cho S, Shin MH, Kim YK *et al.* (2009) Effects of infrared radiation and heat on human skin aging *in vivo*. *J Investig Dermatol Symp Proc* 14:15–9

Elsner P, Wilhelm D, Maibach HI (1990) Mechanical properties of human forearm and vulvar skin. *Br J Dermatol* 122:607–14

Hoshino T, Matsuda M, Yamashita Y *et al.* (2010) Suppression of melanin production by expression of HSP70. *J Biol Chem* 285:13254–63

Imokawa G (2009) Mechanism of UVB-induced wrinkling of the skin: paracrine cytokine linkage between keratinocytes and fibroblasts leading to the stimulation of elastase. *J Investig Dermatol Symp Proc* 14:36–43

Inomata S, Matsunaga Y, Amano S *et al.* (2003) Possible involvement of gelatinases in basement membrane damage and wrinkle formation in chronically ultraviolet B-exposed hairless mouse. *J Invest Dermatol* 120:128–34

Kessenbrock K, Plaks V, Werb Z (2010) Matrix metalloproteinases: regulators of the tumor microenvironment. *Cell* 141:52–67

Kim MS, Kim YK, Lee DH *et al.* (2009) Acute exposure of human skin to ultraviolet or infrared radiation or heat stimuli increases mast cell numbers and tryptase expression in human skin *in vivo*. *Br J Dermatol* 160: 393–402

Kobayashi N, Nakagawa A, Muramatsu T *et al.* (1998) Supranuclear melanin caps reduce ultraviolet induced DNA photoproducts in human epidermis. *J Invest Dermatol* 110:806–10

Krappmann D, Wegener E, Sunami Y *et al.* (2004) The IkappaB kinase complex and NF-kappaB act as master regulators of lipopolysaccharide-induced gene expression and control subordinate activation of AP-1. *Mol Cell Biol* 24:6488–500

Matsuda M, Hoshino T, Yamashita Y *et al.* (2010) Prevention of UVB radiation-induced epidermal damage by expression of heat shock protein 70. *J Biol Chem* 285:5848–58

Matsumura Y, Ananthaswamy HM (2004) Toxic effects of ultraviolet radiation on the skin. *Toxicol Appl Pharmacol* 195:298–308

Maytin EV, Wimberly JM, Kane KS (1994) Heat shock modulates UVB-induced cell death in human epidermal keratinocytes: evidence for a hyperthermia-inducible protective response. *J Invest Dermatol* 103:547–53

Morimoto RI, Santoro MG (1998) Stress-inducible responses and heat shock proteins: new pharmacologic targets for cytoprotection. *Nat Biotechnol* 16:833–8

Park KC, Kim DS, Choi HO *et al.* (2000) Overexpression of HSP70 prevents ultraviolet B-induced apoptosis of a human melanoma cell line. *Arch Dermatol Res* 292:482–7

Plumier JC, Ross BM, Currie RW *et al.* (1995) Transgenic mice expressing the human heat shock protein 70 have improved post-ischemic myocardial recovery. *J Clin Invest* 95:1854–60

Rabe JH, Mamelak AJ, McElgunn PJ *et al.* (2006) Photoaging: mechanisms and repair. *J Am Acad Dermatol* 55:1–19

Rijken F, Bruijnzeel PL (2009) The pathogenesis of photoaging: the role of neutrophils and neutrophil-derived enzymes. *J Investig Dermatol Symp Proc* 14:67–72

Schwartz E (1988) Connective tissue alterations in the skin of ultraviolet irradiated hairless mice. *J Invest Dermatol* 91:158–61

Shin MH, Seo JE, Kim YK *et al.* (2012) Chronic heat treatment causes skin wrinkle formation and oxidative damage in hairless mice. *Mech Ageing Dev* 133:92–8

Talwar HS, Griffiths CE, Fisher GJ *et al.* (1995) Reduced type I and type III procollagens in photodamaged adult human skin. *J Invest Dermatol* 105:285–90

Tang D, Kang R, Xiao W *et al.* (2007) The anti-inflammatory effects of heat shock protein 72 involve inhibition of high-mobility-group box 1 release and proinflammatory function in macrophages. *J Immunol* 179:1236–44

Taraboletti G, Sonzogni L, Vergani V *et al.* (2000) Posttranscriptional stimulation of endothelial cell matrix metalloproteinases 2 and 1 by endothelioma cells. *Exp Cell Res* 258:384–94

Trautinger F (2001) Heat shock proteins in the photobiology of human skin. *J Photochem Photobiol B* 63:70–7

Trautinger F, Kindas-Mugge I, Barlan B *et al.* (1995) 72-kD heat shock protein is a mediator of resistance to ultraviolet B light. *J Invest Dermatol* 105:160–2

Tsuji N, Moriwaki S, Suzuki Y *et al.* (2001) The role of elastases secreted by fibroblasts in wrinkle formation: implication through selective inhibition of elastase activity. *Photochem Photobiol* 74:283–90

Tsukahara K, Nakagawa H, Moriwaki S *et al.* (2004) Ovariectomy is sufficient to accelerate spontaneous skin ageing and to stimulate ultraviolet irradiation-induced photoageing of murine skin. *Br J Dermatol* 151:984–94

Tsukahara K, Takema Y, Moriwaki S *et al.* (2001) Selective inhibition of skin fibroblast elastase elicits a concentration-dependent prevention of ultraviolet B-induced wrinkle formation. *J Invest Dermatol* 117:671–7

Visse R, Nagase H (2003) Matrix metalloproteinases and tissue inhibitors of metalloproteinases: structure, function, and biochemistry. *Circ Res* 92:827–39

Weiss YG, Bromberg Z, Raj N *et al.* (2007) Enhanced heat shock protein 70 expression alters proteasomal degradation of IkappaB kinase in experimental acute respiratory distress syndrome. *Crit Care Med* 35: 2128–2138

Wilson N, McArdle A, Guerin D *et al.* (2000) Hyperthermia to normal human skin *in vivo* upregulates heat shock proteins 27, 60, 72i and 90. *J Cutan Pathol* 27:176–82

Zhao R, Bruning E, Rossetti D *et al.* (2009) Extracts from Glycine max (soybean) induce elastin synthesis and inhibit elastase activity. *Exp Dermatol* 18:883–6

Dig Dis Sci (2013) 58:354–362
DOI 10.1007/s10620-012-2350-x

ORIGINAL ARTICLE

# Attenuation of Acetic Acid-Induced Gastric Ulcer Formation in Rats by Glucosylceramide Synthase Inhibitors

**Manabu Nakashita · Hidekazu Suzuki · Soichiro Miura · Takao Taki · Keita Uehara · Tohru Mizushima · Hiroshi Nagata · Toshifumi Hibi**

Received: 10 May 2012 / Accepted: 28 July 2012 / Published online: 24 August 2012


**Abstract**
*Introduction* Ceramide has been suggested to play a role in apoptosis during gastric ulcerogenesis. The present study is designed to investigate whether accumulated ceramide could serve as the effector molecules of ulcer formation in a rat model of acetic acid-induced gastric ulcer.
*Methods* The effect of fumonisin B1, an inhibitor of ceramide synthase, and of *d,l,-threo*-1-phenyl-2-hexadecanoylamino-3-morpholino-1-propanol (PPMP) and N-butyldeoxynojirimycin (NB-DNJ), both inhibitors of glucosylceramide synthase, on the accumulation of ceramide and formation of gastric ulcer were examined in the rat model of acetic acid-induced gastric ulcer.
*Results* Fumonisin B1 attenuated acetic acid-induced gastric ulcer formation, associated with a decrease in the number of apoptotic cells. Our results showed that it is neither the C18- nor the C24-ceramide itself, but the respective metabolites that were ulcerogenic, because PPMP and NB-DNJ attenuated gastric mucosal apoptosis and the consequent mucosal damage in spite of their reducing the degradation of ceramide.
*Conclusion* The ceramide pathway, in particular, the metabolites of ceramide, significantly contributes to acetic acid-induced gastric damage, possibly via enhancing apoptosis. On the other hand, PPMP and NB-DNJ treatment attenuated gastric mucosal apoptosis and ulcer formation despite increasing the ceramide accumulation, suggesting that it was not the ceramides themselves, but their metabolites that contributed to the ulcer formation in the acetic acid-induced gastric ulcer model.

**Keywords** Ceramide · Glucosylceramide inhibitor · Gastric ulcer · Acetic acid · Apoptosis

M. Nakashita · H. Suzuki (✉) · K. Uehara · H. Nagata · T. Hibi
Division of Gastroentrology and Hepatology, Department of Internal Medicine, School of Medicine, Keio University, 35 Shinanomachi, Shinjuku-ku, Tokyo 160-8582, Japan
e-mail: hsuzuki@a6.keio.jp

M. Nakashita · H. Nagata
Department of Internal Medicine, Keiyu Hospital, Yokohama, Japan

S. Miura
Second Department of Internal Medicine, National Defense Medical College, Saitama, Japan

T. Taki
Molecular Medical Science Institute, Otsuka Pharmaceutical Co. Ltd, Tokushima, Japan

T. Mizushima
Faculty of Pharmacy, Keio University, Tokyo, Japan

## Introduction

While many factors have been thought to be involved in the pathogenesis of gastric ulcers, the mechanism of ulcer formation is not yet precisely understood. Gastric mucosal apoptosis is known to be associated with the loss of mucosal integrity and may play an important role in ulcer development [1, 2]. Recently, enhanced apoptosis in the gastric epithelium has been demonstrated to be of pathophysiological importance in various kinds of gastric lesions, such as stress-induced ulcers [1], *Helicobacter pylori*-positive ulcers [3–5], nonsteroidal anti-inflammatory drug (NSAID)-induced ulcers [6], and chemically induced ulcers, such as ethanol-induced ulcers [7, 8]. Inflammatory cytokines, including tumor necrosis factor (TNF)-$\alpha$ and interferon (IFN)-$\gamma$, have been postulated to play a role in gastric mucosal apoptosis [8].

Recent studies have revealed that sphingolipids (ceramide, sphingosine, etc.) are highly bioactive compounds that are involved in diverse cell processes, including cell-to-cell interactions, adhesion, differentiation and oncogenic transformation [9], as well as cell proliferation and apoptosis. Accumulation of the sphingolipid ceramide (Cer) is a well-known phenomenon in cells undergoing apoptosis [10, 11], and ceramide analogues have been reported to induce apoptosis [12]. In addition to their direct action on apoptosis, ceramides have also been suggested to have a role in apoptosis induced by the addition of extracellular agents, such as TNF-$\alpha$ [13, 14], IFN-$\gamma$ [15] or the anti-Fas antibody [16].

Ceramide analogues have been demonstrated in vitro to induce apoptosis in gastric mucosal cell lines. We previously reported that the subserosal injection of phorbol-12-myristate-13-acetate (PMA) resulted in the formation of gastric ulcers in the rat gastric mucosa [17], associated with a significant increase in the cellular contents of ceramides (C18 and C24 ceramide) [18]. The significant ceramide accumulation was thought to have contributed to the PMA-induced tissue damage in that rat model, possibly via enhancing the apoptotic activity in the gastric mucosa, because co-administration of caspase inhibitors or an inhibitor of sphingolipid biosynthesis attenuated the formation of the gastric ulcers, associated with a reduction in the number of apoptotic cells [18]. However, it remains unknown whether the ceramide-induced gastric mucosal damage was evoked specifically only by the PMA injection or whether the ceramide pathway is also, in general, involved in the formation of gastric ulcers induced by various factors. It is also important to elucidate what kind of downstream molecules may be involved in gastric ulcer formation after ceramide activation.

Ceramide is produced from sphingosine (sphinganine) by sphingosine N-acyltransferase (ceramide synthase), which is potentially inhibited by fumonisin B1. Glucosylceramide synthase (GCS) is a ceramide glucosyl transferase that processes the sphingolipid ceramide [19]. This conversion of ceramide to glucosylceramide is prevented by *d,l,-threo*-1-phenyl-2-hexadecanoylamino-3-morpho-lino-1-propanol (PPMP) and N-butyldeoxynojirimycin (NB-DNJ) [20, 21]. The product, glucosylceramide, can be further elaborated with a variety of oligosaccharides to become glycosphingolipids called gangliosides such as GM3 (monosialoganglioside 3) and GD3 (disialoganglioside 3) [19] (Fig. 1).

To answer these questions, we investigated the ceramide formation and induction of apoptosis and gastric mucosal damage during the gastric ulcer formation process using a rat model of acetic acid-induced gastric ulcer, which is a representative experimental model of chronic gastric ulcer. We also examined the effects of two different kinds of glucosylceramide synthase inhibitors on the gastric ulcer formation induced by acetic acid, to investigate whether it was the ceramides themselves or their metabolites that were involved in the pathogenesis of the gastric ulcers.

## Materials and Methods

### Animals and Ulcer Induction

Male Sprague-Dawlay rats, weighing 200–250 g and maintained on standard laboratory chow (Oriental Yeast Mfg., Ltd., Tokyo, Japan) were used for all the experiments. All the animals were handled according to the guidelines of the Animal Research Committee of Keio University School of Medicine. The rats were denied any food for 24 h prior to the experiments, but were allowed access to tap water ad libitum. Gastric ulcers were induced by injection of an acetic acid solution [22]. Vehicle (water) was injected as a control. In brief, the abdomen of the animals, under anesthesia with 30 mg/kg of pentobarbital sodium, was opened via a midline incision. The stomach was exposed and 50 µl of either 20 % acetic acid or vehicle (water) was injected into the subserosa of the anterior wall of the glandular stomach using a microsyringe, followed by closure of the abdomen.

At different time intervals (24, 48, and 72 h) after the injection of acetic acid or vehicle, the rats were sacrificed with an overdose of sodium pentobarbital. Their stomachs were quickly removed, opened along the greater curvature, and rinsed with cold normal saline. The surface area of each lesion in the gastric mucosa was assessed visually by macroscopic examination. The ulcer area was calculated as an area of similarity ellipse (ulcer area = $\pi^*a^*b^*1/4$; $a$ major axis, $b$ minor axis).

### Administration of Various Inhibitors

To examine the changes in the gastric mucosal ceramide contents in this model, an inhibitor of sphingolipid biosynthesis, fumonisin B1 (FB1), was injected concomitantly (0.036–0.09 g/kg body weight) (Sigma) [23] with the acetic acid into the gastric subserosa. To determine the role of glucosylceramide in the acetic acid-induced ulcer formation, we used two types of inhibitors of glucosylceramide synthase, namely, *d,l,-threo*-1-phenyl-2-hexadecanoylamino-3-morpholino-1-propanol (PPMP) (0.0127–1.27 g/kg body weight) (Sigma-Aldrich) and N-butyldeoxynojirimycin (NB-DNJ) (0.11–11 g/kg body weight) (Sigma-Aldrich), which prevent the conversion of ceramide to glucosylceramide [20, 21]. These inhibitors were also injected concomitantly with acetic acid into the gastric subserosa. To prevent any systemic effects of the ceramide inhibitors as well as any